Artemisia annua tea drug interactions: new method development

A Report for a Major Qualifying Project

Submitted to the Faculty of

WORCESTER POLYTECHNIC INSTITUTE

in fulfillment of the requirements

for the Degree of Bachelor of Science

By

Russell Kam and Ryan Polansky

Advised by

Professor Pamela Weathers and Professor Suzanne Scarlata

Acknowledgements

We would like to thank our families for enabling us to go to Worcester Polytechnic Institute, as well as the members of the Weathers lab, for their patience and well-reasoned feedback.

Abstract

Artemisia annua L. is a medicinal herb used in traditional Chinese medicine and the source of artemisinin, a component of a current leading antimalarial treatment. Traditionally, *Artemisia annua* tea has been used as a treatment for a variety of illnesses including malaria. However, artemisinin has been shown to inhibit P450 CYP3A4, which metabolizes approximately half of clinically used drugs today. Among those drugs are caffeine and acetaminophen, household staples that also inhibit CYP3A4 in great enough quantities. A previous MQP used Promega's P450-glo assays to analyze the interactions of those drugs with each other to determine, among other things, the safety of taking *A. annua* tea alongside either of the other two drugs. However, due to time and cost restraints, they were unable to analyze the full range of data necessary to make the proper analysis. In this MQP, we looked at using a 7-Benzyloxy-4-(trifluoromethyl) coumarin (BFC) based fluorescence assay in order to achieve similar results with a significantly reduced cost and equal convenience to the P45-glo assay. The first step was using the BFC assay to analyze the metabolism of BFC by CYP3A4 when in the presence of ketoconazole, a known CYP3A4 inhibitor, so as to independently confirm the assay's consistency and suitability for use in the lab. Following that, the team used the assay to analyze *A. annua* tea, with the goal of performing assays on mixtures of *A. annua* tea with acetaminophen or caffeine, as the prior MQP did, but on a larger scale so as to confirm or deny their results using a wider range of concentrations. However, as we progressed through our investigation, we determined that the *A. annua* tea had an inherent fluorescence that was challenging the assay. By measuring the background fluorescence of the extract and subtracting it from the final fluorescence the assay was useful in analysis of CYP 3A4 activity in the BFC assay and may be useful in further studies subsequent to this project in measuring drug interactions with *A. annua* tea.

Table of Contents

1.0 Background

1.1 *Artemisia annua* tea (rp)

1.1.1 Overview (rp)

Artemisia annua L. (Figure 1a) is an annual herb that is used in traditional Chinese medicine for the purpose of making medicinal tea and was investigated for medical use in a modern context for the sake of combating malaria (Millet et al., 2011). Its active ingredient, artemisinin (Figure 1b), was derivatized to make the molecule more bioavailable; artemisinin derivatives include artesunate, artemether, arteether, and dihydroartemisinin. They are the primary drugs of choice used in malaria treatments, alongside other antimalarial drugs taken in combination to reduce the emergence of artemisinin resistance (Cui et al., 2009). Despite this,

A:

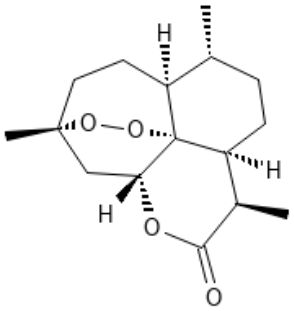

B:

Figure1: (A) An *Artemisia annua* plant growing in our lab. (B) Structure of Artemisinin.

Artemisinin Combination Therapy (ACT) can be expensive and inaccessible, sometimes prohibitively so, as for a family of four living on a subsistence income of approximately $300-$600 annually, even $6-$8 is a significant amount of money, particularly when malaria can be caught repeatedly. Cost and accessibility lead many in low- and middle-income countries

(LIMC) to seek a more traditional alternative, sometimes not just for malaria, but other illnesses and ailments as well, against which artemisinin and *A. annua* have demonstrated to have at least some degree of efficacy (Weathers 2023).

The promotion or use of plant material from any *Artemisia* species, including *A. annua*, as antimalarial medication is not supported by the World Health Organization (WHO) for a variety of reasons, which they cite as highly variable content, the potential hastening and spread of artemisinin resistance, and the presence of ACT treatments (World Health Organization, 2019). However, the WHO's stance on the matter and the reasons given are not consistent with the current research on the topic: for instance, there is no evidence of *A. annua* eliciting artemisinin resistance (Weathers et al., 2022) (Elfawal et al., 2015). Regardless of the politics, it *is* still used successfully, and consequently, the study of its interactions with other widely available and frequently used drugs, such as caffeine and acetaminophen, is valuable to understand the potential risks, or lack thereof, of taking both concurrently.

This topic was previously the subject of a prior MQP with the intent of filling in some missing gaps (Duncan & Togneri, 2023). They reported CYP3A4 MIC and IC_{50} values using a Promega P450-Glo luminescence assay. While the prior group tested concentrations of caffeine, acetaminophen, in combination with *A. annua* tea for interaction with CYP3A4 the team determined that *A. annua* tea likely had inhibitory reactions with both drugs. However, they were unable to test the full range of either drug because of assay costs and a desire to focus more on realistic concentrations of each drug that a human would consume. To provide those missing data, we are endeavoring to validate a different assay system that is more affordable to facilitate testing a broader range of each drug with *A. annua* tea.

1.1.2 Artemisinin (rk)

Artemisinin (Figure 1b) is primarily metabolized by the cytochrome P450 liver enzyme, CYP2B6, with minor hepatic metabolism by CYP3A4 (Gordi et al., 2005). The metabolic liver processing of artemisinin produces various compounds including deoxyartemisinin, deoxydihydroartemisinin, and 9,10-dihydrodeoxyartemisinin (Lee and Hufford, 1990). However, these metabolites are physiologically inert as they do not contain artemisinin's peroxide group (Lee and Hufford, 1990). Therefore, use of *A. annua* should not involve any harsh chemical treatments to protect its peroxide group. Indeed, isolated artemisinin (the active ingredient) has shown fewer synergistic effects than *A. annua* tea (Cai et al., 2017)

1.1.3 *Artemisia annua* (rk & rp)

A. annua, also known by its various common names, such as sweet wormwood, sweet annie, and annual wormwood, is an annual herbaceous herb and a member of the *Asteraceae* family, which also, of note, includes sunflowers, mugwort, dandelions, milk thistle, etc. (Powers 2023). *A. annua* is grown across Eurasia, as well as in the more temperate regions of Africa, Australia, and the Americas (Septembre-Malaterre et al., 2020). In addition to the already-noted

medicinal uses as tea infusions, the plant has also been historically used as a dietary spice and for herbal teas beyond medicinal purposes (Septembre-Malaterre et al., 2020). There are Chinese and Vietnamese records going as far back as the second century BCE showing medicinal use of *A. annua*. While ancient physicians had trouble with extraction they created an emulsified mixture of flavonoids, oils, and plant matter in water by soaking and wringing the plant. However, there are recordings of the plant's juice being ingested instead of as a tea or as the aforementioned mixture (Tu, 2011). Today, *A. annua*'s antimalarial effects have taken the spotlight but there are records of Chinese physicians using *A. annua* to relieve boils, bug bites and hemorrhoids as well as treating fevers (Hsu, 2006). Despite all this, there is modern debate about the efficacy of *A. annua*'s antimalarial effects as the WHO disapproves of its antimalarial use (World Health Organization, 2019). However, the political side of this matter has already been noted in section 1.1.1.

1.2 Acetaminophen (rp)

Acetaminophen (APAP), a phenolic, often sold under the brand name of Tylenol, is a widely used drug and according to some studies, the one most frequently used in the United States, (McGill and Jaeschke, 2013). In 2008, over 20 billion doses were sold (Krenzelok, 2009). APAP is used primarily to treat fevers and reduce pain, and is normally safe and effective; however, it can cause liver damage when one overdoses on it by taking more than 4 grams over a 24-hour period (McGill and Jaeschke, 2013). With that in mind, the question of how APAP interacts with *A. annua* tea becomes especially important, as, depending on the exact nature of their interactions, it is entirely possible that taking them concurrently could lead to an ordinarily safe dose of APAP becoming toxic.

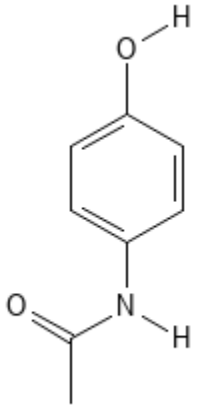

Figure 2: Structure of acetaminophen (APAP).

1.2.1 Metabolism of Acetaminophen (rk)

While acetaminophen (APAP) has a high bioavailability of 88%, when it is ingested only 5% of it remains intact with roughly 95% of the ingested APAP metabolized by the liver (Figure

3). When hepatic CYP3A4 catalyzes oxidation of APAP there are three main metabolite categories formed: 52-57% becomes pharmacologically inactive glucuronides (APAP-gluc), 30-44% become pharmacologically inactive sulfur conjugates (APAP-sulfates) and 5-10% become N-acetyl-p-benzoquinone imine (NAPQI), which is pharmacologically reactive (Mazaleuskaya et al., 2015). When there is an excess of NAPQI, it begins to covalently bind to proteins that can eventually lead to APAP toxicity. Additionally, other small molecule drugs can amplify APAP's liver toxicity and later damage the liver. A prime example of this is many epileptic drugs such as

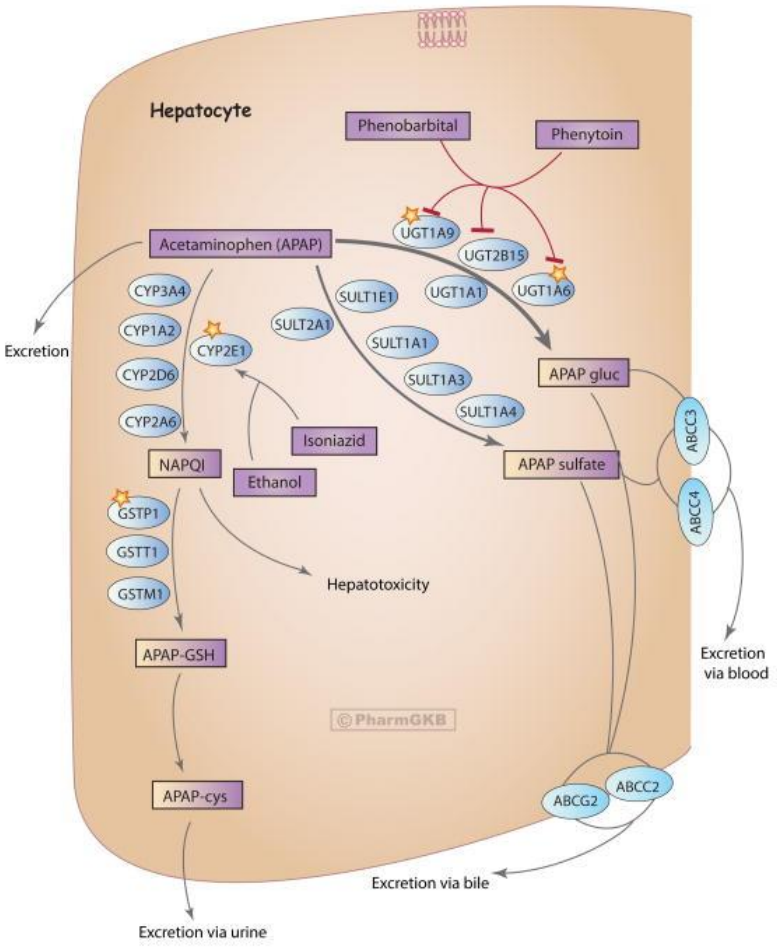

Figure 3: Metabolic pathway of acetaminophen's oxidation via hepatic CYPs and other hepatic enzymes (Mazaleuskaya, 2015).

phenytoin or phenobarbital. Those drugs increase APAP toxicity by inhibiting various enzymes in the UGT family, another xenobiotic metabolizing family of enzymes. When enzymes in the UGT family are inhibited, there is increased systematic exposure of co-administered drugs as well as lowered metabolism leading to larger amounts of NAQPI with subsequent hepatotoxicity (Kostrubsky et al., 2005).

1.3 Caffeine (rp)

Caffeine (CAF), a methylxanthine drug (Figure 4) is, in many ways, essentially ubiquitous: it is in some of the most widely-consumed beverages — coffee, *Camelia sinensis* tea (includes white, yellow, green, and red/black tea), and many soft drinks. Over 85% of adults and about 75% of children in the US consume it regularly (Temple et al., 2017). Practically speaking, CAF is a stimulant, frequently used for increasing a user's energy, level of alertness, and ability to concentrate; however, high doses, in excess of the equivalent of four cups of coffee, can lead to symptoms such as insomnia, anxiety, and elevated heart rate (Nehlig, 1997). Overall, while those symptoms are generally much less damaging than the effects of an APAP overdose, they still have a dramatic effect on quality of life. Additionally, the interactions between artemisinin and CAF could lead to a significantly worse outcome for a user.

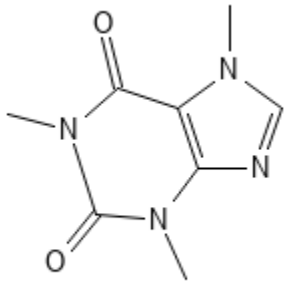

Figure 4: Structure of caffeine (CAF).

1.3.1 Metabolism of Caffeine (rk)

While CAF is metabolized in the liver by CYP3A4, it is primarily metabolized by CYP1A2 into paraxanthine with varying efficiency among individual humans (Figure 5). The range of difference can be up to an order of magnitude more efficient. This difference in activity of CYP1A2 can vary 5 to 15-fold and is assumed to be a result of both genetic and environmental factors (Urry et al., 2016). However, CAF metabolism is complex as it involves multiple enzymes and has upwards of 20 observed metabolites (Figure 5; Sevrioukova, 2023). CAF can bind to multiple sites within CYP3A4 and is also capable of multiple substrate binding. It is posited that CAF modulates enzymatic activity of CYP3A4 (Sevrioukova, 2023). Additionally, CAF has some observed drug-drug interactions (Sevrioukova, 2023). Indeed, CAF has a wide variety of caffeine-drug interactions as well as caffeine-caffeine interactions. For example, CAF has been observed creating "π-π stacking complexes between caffeine and polyaromatic pharmaceuticals, such as daunomycin, doxorubicin, and mitoxantrone" where it reduces the bonded drugs' chemical availability (Sevrioukova, 2023). Additionally, caffeine has been shown to dimerize and polymerize, which is hypothesized to be chemically unpredictable but important to cell function although it is largely unstudied (Sevrioukova, 2023). However, some caffeine-caffeine compounds have been studied directly binding to a variety of enzyme's

active site but this interaction and its effect on CYP3A4 xenobiotic metabolism are still largely unknown.

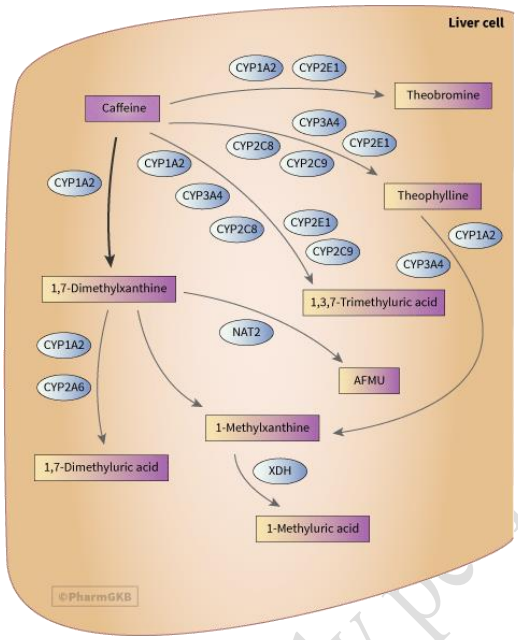

Figure 5: Metabolic Pathway of CAF by CYPs and other hepatic enzymes (Mazaleuskaya, 2015)

1.4 CYP3A4 Herb Assays (rp)

There is already considerable literature on many methods for studying activity of CYP3A4 that can be used to also measure interactions with medicinal herbs (Table 1). While the list of methods in Table 1 is not exhaustive, it does display the information from a fair number of papers, many of which measured quite different things. Generally, there is one of two primary factors measured when looking at the interaction between CYP3A4 and medicinal herbs: the inhibition of CYP3A4, or the modulation of CYPP450 production. For example, in Al-Dosari and Parvez (2018) 58 different plants were screened for changes in CYP3A4 activity. Extracts from four of those species induced production of CYP3A4: *Ficus palmata*, *Euphorbia tirucalli*, *Dodonaea angustifolia*, and *Alternanthera pungens* (Al-Dosari and Parvez, 2018). In that study, they measured induction of CYP3A4 in 80% ethanol extracts via a luciferase gene reporter assay, using firefly luciferase as the reporter in a cell culture and normalizing it to renilla luciferase. In another instance, Mazzai et al. used qPCR and measured the induction of CYP3A4 transcripts in four native Brazilian medicinal plant extracts, with *Solanum paniculatum* the only species that inhibited CYP3A4's induction (Mazzari et al., 2016).

Table 1: Examples of methods used in other CYP3A4-Herb studies..

Assay method	Ref.
7-Benzyloxyquinine Fluorescence Assay, using plant succus, a traditional method of preparing herbal medicine	(Larson et al., 2016)
7-Benzyloxyquinine Fluorescence Assay, using a methanol extract	(Larson et al., 2014)
High Performance Liquid Chromatography (HPLC)	(Kondža et al., 2023)
HPLC	(Georgiev et al., 2019)
HPLC, primarily of testosterone 6β-hydroxylation	(Sunaga et al., 2012)
Liquid chromatography–mass spectrometry (LCMS)	(Yilue et al., 2019)
Promega P450-Glo CYP3A4 Assays	(Ashour et al., 2019; Desrosiers et al., 2020)
Promega Dual-Luciferase Reporter Assays	(Al-Dosari and Parvez, 2018)
RT-qPCR or the associated gene	(Mazzari et al., 2016)
Ultra-performance liquid chromatography–mass spectrometry (UPLCMS)	(Feltrin et al., 2020)

Unlike Al-Dosari and Parvez, who made 50 µg/mL ethanol extracts via grinding up the components before going through cycles of suspension and resuspension, Mazzari et al. made infusions of the herbs for 20 min, although neither the temperature nor the solvent was specified. In another report, investigators focused on developing a Caco-2 based assay for measuring CYP3A4 and CYP2D6 activity, in response to extracts of *Cecropia glaziovii*, *Ilex paraguariensis*, *Bauhinia forficata*, and an *Echinacea* species, on their activity (Feltrin et al., 2019). Those results showed that Caco-2 based fluorescence assays were a potential and viable route for studying CYP3A4 induction. However, Caco-2 cells are intestinal cells and thus not directly applicable to liver metabolism of artemisinin.

The focus of many of the studies was not induction, but inhibition, measured as an IC_{50}, the percentage of activity remaining after exposure to a certain herb, or the percent inhibition caused by a given herb. The largest study was that by Ashour et al. that measured data with the latter criterion (Ashour et al., 2019). In that study, they used Promega P450-glo assays to analyze the inhibition of CYP3A4 caused by aqueous and methanol extracts of 57 different herbs used in Traditional Chinese Medicine, checking three different concentrations of each: 1000, 200, and 100 µg/mL for the aqueous extract, and 500, 200, and 100 µg/mL for the methanol extract.

Table 2: Interactions of CYP3A4 with various plant extracts.

Herb	Measure	Type	Source
Abrus cantoniensis	22.40 ± 2.65%	Inhibition in 100 µg/mL refluxed water extract	(Ashour et al., 2019)
	19.29 ± 2.78%	Inhibition in 100 µg/mL refluxed methanol extract	
Acacia catechu	96.01 ± 5.92%	Inhibition in 100 µg/mL refluxed water extract	
	62.34 ± 3.40%	Inhibition in 100 µg/mL refluxed methanol extract	
Andrographis paniculata	87.57 ± 3.62%	Inhibition in 100 µg/mL refluxed water extract	
	17.65 ± 2.56%	Inhibition in 100 µg/mL refluxed methanol extract	
Alpinia galanga	24.92 ± 4.19%	Inhibition in 100 µg/mL refluxed water extract	
	52.53 ± 2.18%	Inhibition in 100 µg/mL refluxed methanol extract	
Alternanthera pungens	1.74 fold	Induction in 50 µg/mL ethanol extract	(Al-Dosari and Parvez, 2018)
Arctium lappa	93.47 ± 5.93%	Inhibition in 100 µg/mL refluxed water extract	(Ashour et al., 2019)
	47.92 ± 3.66%	Inhibition in 100 µg/mL refluxed methanol extract	
Areca catechu	98.94 ± 6.24%	Inhibition in 100 µg/mL refluxed water extract	
	56.94 ± 4.35%	Inhibition in 100 µg/mL refluxed methanol extract	
Artemisia afra	5.59 µM	IC_{50} in tea	(Desrosiers et al., 2020)
Artemisia annua	83.96 ± 4.62%	Inhibition in 100 µg/mL refluxed water extract	(Ashour et al., 2019)
	31.01 ± 3.98%	Inhibition in 100 µg/mL refluxed methanol extract	
	5.67 µM	IC_{50} in tea	(Kondža et al., 2023)
	5.67 µM	IC_{50} in tea	(Desrosiers et al., 2020)
Artemisia capillaris	82.36 ± 5.40%	Inhibition in 100 µg/mL refluxed water extract	(Ashour et al., 2019)
	33.95 ± 2.27%	Inhibition in 100 µg/mL refluxed methanol extract	
Belamcanda chinensis	85.90 ± 2.05%	Inhibition in 100 µg/mL refluxed water extract	
	42.99 ± 2.55%	Inhibition in 100 µg/mL refluxed methanol extract	
Bupleurum marginatum	96.98 ± 3.14%	Inhibition in 100 µg/mL refluxed water extract	
	47.21 ± 3.15%	Inhibition in 100 µg/mL refluxed methanol extract	
Calophyllum inophyllum	79%	Inhibition with 100 µM succus	(Larson et al., 2016)
	79%	Inhibition with 100 µM methanol extract	(Larson et al., 2014)
Camellia sinensis (*Bancha* green tea)	1.35 mg/mL	IC_{50} of extracted methylxanthines	(Georgiev et al., 2019)
Camellia sinensis (*Pu-erh* green tea)	1.28 mg/mL	IC_{50} of extracted methylxanthines	
Capsella bursa-pastoris	17.13 ± 4.64%	Inhibition in 100 µg/mL refluxed water extract	(Ashour et al., 2019)
	7.35 ± 3.22%	Inhibition in 100 µg/mL refluxed methanol extract	
Cassia alata	62%	Inhibition with 100 µM succus	(Larson et al., 2016)
	57%	Inhibition with 100 µM methanol extract	(Larson et al., 2014)
Cassia tora	58.72 ± 3.70%	Inhibition in 100 µg/mL refluxed water extract	(Ashour et al., 2019)

	16.38 ± 3.08%	Inhibition in 100 µg/mL refluxed methanol extract	
Casuarina equisetifolia	74%	Inhibition with 100 µM succus	(Larson et al., 2016)
	61%	Inhibition with 100 µM methanol extract	(Larson et al., 2014)
Celosia cristata	37.38 ± 3.99%	Inhibition in 100 µg/mL refluxed water extract	(Ashour et al., 2019)
	1.79 ± 1.02%	Inhibition in 100 µg/mL refluxed methanol extract	
Centella asiatica	64.16 ± 2.40%	Inhibition in 100 µg/mL refluxed water extract	
	22.89 ± 3.22%	Inhibition in 100 µg/mL refluxed methanol extract	
Centipeda minima	75.33 ± 5.71%	Inhibition in 100 µg/mL refluxed water extract	
	12.14 ± 3.05%	Inhibition in 100 µg/mL refluxed methanol extract	
Cecropia glaziovii	102.1 µg/mL	IC_{50} in aqueous extract	(Feltrin et al., 2020)
Chrysanthemum indicum	89.88 ± 3.91%	Inhibition in 100 µg/mL refluxed water extract	(Ashour et al., 2019)
	46.18 ± 4.99%	Inhibition in 100 µg/mL refluxed methanol extract	
Chrysanthemum morifolium	79.67 ± 5.06%	Inhibition in 100 µg/mL refluxed water extract	
	41.00 ± 4.26%	Inhibition in 100 µg/mL refluxed methanol extract	
Cnidium monnirei	59.79 ± 3.51%	Inhibition in 100 µg/mL refluxed water extract	
	1.51 ± 1.46%	Inhibition in 100 µg/mL refluxed methanol extract	
Cronton tiglium	71.14 ± 4.64%	Inhibition in 100 µg/mL refluxed water extract	
	16.86 ± 3.14%	Inhibition in 100 µg/mL refluxed methanol extract	
Cymbopogon distans	14.72 ± 2.21%	Inhibition in 100 µg/mL refluxed water extract	
	2.71 ± 1.53%	Inhibition in 100 µg/mL refluxed methanol extract	
Cynanchum paniculatum	27.95 ± 3.90%	Inhibition in 100 µg/mL refluxed water extract	
	22.62 ± 3.62%	Inhibition in 100 µg/mL refluxed methanol extract	
Cyrtomium fortune	74.91 ± 3.39%	Inhibition in 100 µg/mL refluxed water extract	
	15.47 ± 4.11%	Inhibition in 100 µg/mL refluxed methanol extract	
Dendrobium loddigesii	64.47 ± 1.40%	Inhibition in 100 µg/mL refluxed water extract	
	4.44 ± 2.37%	Inhibition in 100 µg/mL refluxed methanol extract	
Desmodium styracifolium	11.16 ± 2.78%	Inhibition in 100 µg/mL refluxed water extract	
	10.22 ± 3.12%	Inhibition in 100 µg/mL refluxed methanol extract	
Dodonaea angustifolia	2.62 fold	Induction in 50 µg/mL ethanol extract	(Al-Dosari and Parvez, 2018)
Dysosma versipellis	93.49 ± 4.60%	Inhibition in 100 µg/mL refluxed water extract	(Ashour et al., 2019)
	5.97 ± 2.88%	Inhibition in 100 µg/mL refluxed methanol extract	
Eclipta prostata	54.43 ± 3.51%	Inhibition in 100 µg/mL refluxed water extract	
	14.49 ± 2.02%	Inhibition in 100 µg/mL refluxed methanol extract	

Eleutherococcus senticosus	51.73 ± 2.30%	Inhibition in 100 µg/mL refluxed water extract	
	29.03 ± 4.51%	Inhibition in 100 µg/mL refluxed methanol extract	
Equisetum hiemale	21.99 ± 3.11%	Inhibition in 100 µg/mL refluxed water extract	
	20.49 ± 3.09%	Inhibition in 100 µg/mL refluxed methanol extract	
Euphorbia tirucalli	1.95 fold	Induction in 50 µg/mL ethanol extract	(Al-Dosari and Parvez, 2018)
Euterpe oleracea	28.03 µg/µl	IC_{50} in methanol extract	(Yilue et al., 2019)
Evodia lepta	31.27 ± 2.48%	Inhibition in 100 µg/mL refluxed water extract	(Ashour et al., 2019)
	42.95 ± 3.82%	Inhibition in 100 µg/mL refluxed methanol extract	
Evodia rutaecarpa	14.27 ± 3.07%	Inhibition in 100 µg/mL refluxed water extract	
	32.85 ± 4.25%	Inhibition in 100 µg/mL refluxed methanol extract	
Ficus palmata	1.65 fold	Induction in 50 µg/mL ethanol extract	(Al-Dosari and Parvez, 2018)
Grapefruit Juice (*Citrus paradisi*)	14.4 ± 1.8% of control	Activity after 20 min in 20% ethyl acetate extract	(Sunaga et al., 2012)
Harpagophytum procumbens	29.66 ± 2.88%	Inhibition in 100 µg/mL refluxed water extract	(Ashour et al., 2019)
	15.56 ± 3.13%	Inhibition in 100 µg/mL refluxed methanol extract	
Hedyotis diffusa	9.29 ± 2.34%	Inhibition in 100 µg/mL refluxed water extract	
	25.49 ± 3.91%	Inhibition in 100 µg/mL refluxed methanol extract	
Houttuynia cordata	15.76 ± 3.94%	Inhibition in 100 µg/mL refluxed water extract	
	24.26 ± 3.69%	Inhibition in 100 µg/mL refluxed methanol extract	
Ilex paraguariensis	124.2 µg/mL	IC_{50} in 1:1 methanol-water extract	(Feltrin et al., 2020)
Ipomoea pes-caprae	70%	Inhibition with 100 µM succus	(Larson et al., 2016)
	60%	Inhibition with 100 µM methanol extract	(Larson et al., 2014)
Isatis indigotica	23.96 ± 4.41%	Inhibition in 100 µg/mL refluxed water extract	(Ashour et al., 2019)
	19.99 ± 3.21%	Inhibition in 100 µg/mL refluxed methanol extract	
Kadsura longipedunculata	49.55 ± 3.16%	Inhibition in 100 µg/mL refluxed water extract	
	48.30 ± 4.70%	Inhibition in 100 µg/mL refluxed methanol extract	
Lepidium meyenii	32.73 µg/µl	IC_{50} in methanol extract	(Yilue et al., 2019)
Lonicera confusa	60.91 ± 7.46%	Inhibition in 100 µg/mL refluxed water extract	(Ashour et al., 2019)
	0.44 ± 0.27%	Inhibition in 100 µg/mL refluxed methanol extract	
Lycopersicon esculentum (Squeezed whole tomato)	30.1 ± 3.9%	Activity after 20 min in ethyl acetate extract	(Sunaga et al., 2012)
Lycopersicon esculentum (Tomato Juice A)	29.8 ± 0.1%	Activity after 20 min in 20% ethyl acetate extract	
Lycopersicon esculentum (Tomato Juice B)	25.8 ± 1.7%	Activity after 20 min in 20% ethyl acetate extract	

Lycopersicon esculentum (Tomato Juice C)	16.5 ± 3.1%	Activity after 20 min in 20% ethyl acetate extract	
Magnolia officinalis	58.68 ± 5.96%	Inhibition in 100 µg/mL refluxed water extract	(Ashour et al., 2019)
	14.85 ± 0.62%	Inhibition in 100 µg/mL refluxed methanol extract	
Mahonia bealei	35.54 ± 4.31%	Inhibition in 100 µg/mL refluxed water extract	
	56.72 ± 4.93%	Inhibition in 100 µg/mL refluxed methanol extract	
Mentha haplocalyx	52.15 ± 4.91%	Inhibition in 100 µg/mL refluxed water extract	(Ashour et al., 2019)
	1.19 ± 0.37%	Inhibition in 100 µg/mL refluxed methanol extract	
Ophioglossum vulgatum	60.86 ± 5.09%	Inhibition in 100 µg/mL refluxed water extract	
	24.91 ± 0.54%	Inhibition in 100 µg/mL refluxed methanol extract	
Panax notoginseng	44.91 ± 5.41%	Inhibition in 100 µg/mL refluxed water extract	
	29.83 ± 3.86%	Inhibition in 100 µg/mL refluxed methanol extract	
Paris polyphylla	4.08 ± 2.19%	Inhibition in 100 µg/mL refluxed water extract	
	2.92 ± 1.18%	Inhibition in 100 µg/mL refluxed methanol extract	
Passiflora foetida	64 ± 5%	Inhibition with 100 µM succus	(Larson et al., 2016)
	51%	Inhibition with 100 µM methanol extract	(Larson et al., 2014)
Patrinia scabiosaefolia	37.78 ± 3.69%	Inhibition in 100 µg/mL refluxed water extract	(Ashour et al., 2019)
	0.61 ± 0.04%	Inhibition in 100 µg/mL refluxed methanol extract	
Polygonum cuspidatum	74.20 ± 8.05%	Inhibition in 100 µg/mL refluxed water extract	
	39.81 ± 4.68%	Inhibition in 100 µg/mL refluxed methanol extract	
Polygonum multiflorum	40.41 ± 2.49%	Inhibition in 100 µg/mL refluxed water extract	
	18.02 ± 3.41%	Inhibition in 100 µg/mL refluxed methanol extract	
Punica granatum	33.48 ± 4.75%	Inhibition in 100 µg/mL refluxed water extract	
	16.76 ± 2.18%	Inhibition in 100 µg/mL refluxed methanol extract	
Rosa laevigata	37.37 ± 3.53%	Inhibition in 100 µg/mL refluxed water extract	
	21.52 ± 3.73%	Inhibition in 100 µg/mL refluxed methanol extract	
Sanguisorba officinalis	83.94 ± 7.95%	Inhibition in 100 µg/mL refluxed water extract	
	59.96 ± 3.52	Inhibition in 100 µg/mL refluxed methanol extract	
Saposhnikovia divaricata	13.69 ± 1.51%	Inhibition in 100 µg/mL refluxed water extract	
	8.21 ± 3.14%	Inhibition in 100 µg/mL refluxed methanol extract	
Scutellaria baicalensis	59.43 ± 3.90%	Inhibition in 100 µg/mL refluxed water extract	
	20.55 ± 4.91%	Inhibition in 100 µg/mL refluxed methanol extract	
Selaginella	36.23 ± 2.13%	Inhibition in 100 µg/mL refluxed water extract	

tamariscina	28.89 ± 1.93%	Inhibition in 100 µg/mL refluxed methanol extract	
Senecio scandens	61.07 ± 4.98%	Inhibition in 100 µg/mL refluxed water extract	
	15.80 ± 3.14%	Inhibition in 100 µg/mL refluxed methanol extract	
Siegesbeckia orientalis	22.79 ± 2.17%	Inhibition in 100 µg/mL refluxed water extract	
	28.76 ± 4.82%	Inhibition in 100 µg/mL refluxed methanol extract	
Sida rhombifolia	60%	Inhibition with 100 µM succus	(Larson et al., 2016)
Solanum paniculatum	2.4 fold	Expression inhibition in 100 µg/mL extract	(Mazzari et al., 2016)
Spatholobus suberectus	91.50 ± 7.65%	Inhibition in 100 µg/mL refluxed water extract	(Ashour et al., 2019)
	36.42 ± 2.13%	Inhibition in 100 µg/mL refluxed methanol extract	
Taxillus chinensis	61.50 ± 5.69%	Inhibition in 100 µg/mL refluxed water extract	
	47.41 ± 1.07%	Inhibition in 100 µg/mL refluxed methanol extract	
Terminalia catappa	87%	Inhibition with 100 µM succus	(Larson et al., 2016)
	80%	Inhibition with 100 µM methanol extract	(Larson et al., 2014)
Verbena officinalis	11.85 ± 2.10%	Inhibition in 100 µg/mL refluxed water extract	(Ashour et al., 2019)
	9.54 ± 3.26%	Inhibition in 100 µg/mL refluxed methanol extract	
Viola yezoensis	9.29 ± 4.67%	Inhibition in 100 µg/mL refluxed water extract	
	24.97 ± 2.75%	Inhibition in 100 µg/mL refluxed methanol extract	

Only the 100 µg/mL aqueous extract data were included in Table 2, primarily due to space concerns, it was the concentration most analyzed by the paper, and the aqueous extracts tended to have higher inhibitions than the methanol ones. Unfortunately, Ashour et al. did not explain their rationale for using different extract concentration ranges. Instead of using fluorescence-based assays, the majority of studies on herbal inhibition of CYP3A4 seem to have used chromatography assays, directly analyzing the products resulting from CYP3A4 metabolism of specific substrates. For instance, Sunaga et al.(2012) used three different substrates, testosterone, nifedipine, and midazolam, to measure CYP3A4 activity in ethyl acetate extracts of tomato juice. Although they used three substrates, the majority of their data reported the 6β-hydroxylation of testosterone (Sunaga et al., 2012). This approach, compared to using fluorescence-based assays, has the potential to allow for more specific measurements, particularly when the herbal extract being used is itself fluorescent. However, unlike when performing chromatography with pure chemicals, there is a lot of potential interference when using herbal extracts, particularly if the specific composition of the extract is unknown. Fluorescence-based assays, consequently, can be considered to be more generally reliable than chromatography assays for analyzing the effect of herbal medicines on CYP3A4.

While the above table does not deal with interactions between different drugs, it does look at the essential first component to determining that: how the drugs operate on their own.

The data produced by the numerous studies on the topic, looking at, primarily, inhibition, provides a good start point for interaction studies, such as via a checkerboard assay.

1.5 Measuring drug-drug interactions (rp)

People do not always take one drug at a time. Even if when taking multiple drugs they do so individually, the drugs themselves or any number of biological derivatives of them may chemically interact. Drugs may be consumed concurrently or in near time proximity to one another such that the pharmacokinetics (PK) and pharmacodynamics (PD) of the drugs create an interaction. Indeed, because of the peripheral blood system, two drugs may cause activity in the same parts of the body without either being near that part of the body or each other.

Regardless of the means through which different drugs, or at least the effects of different drugs, come into contact, they do not always simply produce their effects separately. Frequently, they interact with one another in ways that are either synergistic where one or both drugs augment the effects of the other, or antagonistic where one or both drugs counteract the other (Bijnsdorp 2011). There can be merits and demerits to both, depending on the specifics. For instance, a synergistic pair of drugs could produce an effect equivalent to a larger amount for a reduced cost, but more action is not necessarily beneficial: overdosing would be more likely even if both drugs were used safely and responsibly. Meanwhile, while an antagonistic combination could lead to wasted resources, it could also involve one drug suppressing the detrimental side effects of another, leading to a result that is safer overall. To determine whether a drug combination is safe or healthy in each combination, one must understand how those drugs interact, if at all

To attain that understanding, one first establishes how each drug works in insolation and establish its minimum inhibitory concentration (MIC), then combinations of drugs are tested on biological components they would normally affect, whether those components are whole cells, entire organisms, or artifacts of destroyed cells like microsomes. The combination's effect is quantified and compared against the effects of each drug individually on the given components. The discrepancy, or lack thereof, is used to determine if the interactions, if extant, are synergistic, antagonistic or independent of one another.

1.5.1 Checkerboard Assay (rp)

A Diagonal Checkerboard Assay is used for interaction studies. This assay has advantages over other assay methods when studying the interaction between two different chemicals within a given assay and can even be used in a multi-plate setup to effectively measure the interactions between three different chemicals (Cokol-Cakmak et al., 2018). The primary idea behind this assay is to have a pair of gradients, one for each drug, up and down the x and the y axes of the plate, thus causing each well to have a different ratio of each chemical, while also reducing tedium in the process of filling the wells in question.

This assay can have three overall results, as determined by the pattern of the "checkerboard," and perhaps most importantly, shape of the contour of the well results (Cokol-Cakmak et al., 2018). In cases where the contour is straight, the two drugs that aren't varying within a given plate have additive interactions, indicating no significant difference or interaction between the drugs. When the shape is convex, however, a synergistic interaction is apparent, indicating that the interaction of the two drugs enhances the activity of the reporter. Finally, when the shape is concave, they're antagonistic drugs, meaning that their interaction inhibits the reporter to a lesser degree than either individually.

1.6 Enzyme kinetics (rk)

Enzyme kinetics are typically influenced by three key parameters: the Michaelis constant (K_m), maximal velocity (V_{max}), and the catalytic constant (k_{cat}) (Voet et al., 2016). The Michaelis constant signifies the amount of substrate required for an enzyme to operate at half of its maximum velocity and is closely associated with the enzyme's affinity for a substrate. Maximal velocity is the highest rate at which an enzyme generates product from the substrate when the substrate is in excess in the solution (Voet et al., 2016). The catalytic constant, also known as the turnover number, represents the frequency with which a single active site on an enzyme converts substrate to product within a given time frame (Voet et al., 2016).

These parameters play a crucial role in the Michaelis-Menten Equation, yet a significant aspect remains unexplored: inhibitors. Inhibitors, whether proteins or substances, bind to enzymes, diminishing their productivity. In the Michaelis-Menten Equation, they are represented by the term ($1 + I/K_i$). Various inhibitors exist, each specific to the enzyme to which it binds (Voet et al., 2016,). K_i is the dissociation constant of a complex formed by the enzyme and inhibitor. Another relevant term is the IC_{50} that represents the concentration of inhibitors required to reduce enzyme activity to 50% efficiency. Competitive, noncompetitive, and uncompetitive inhibitors are classified based on how they impact the velocity of the equation.

Competitive inhibition is when the substrate and inhibitor bind at the same active site but are mutually exclusive (Strelow et al., 2012). This is characterized by an increased K_m but no change in V_{max}. With high enough substrate concentrations there can be a relevant increase in K_i. Noncompetitive inhibition is characterized by a decreased V_{max} with no change in K_i or K_m. A high-profile example of competitive inhibition is a protease inhibitor which is a common treatment for hepatitis or HIV/AIDS (Eatemadi et al., 2017). The protease inhibitor blocks the active site of the protease preventing propagation of the virus as the next generation of viruses are created in a long chain.

Noncompetitive inhibition happens when the inhibitor binds to the enzyme at an allosteric site which means it is not the active site preventing substrate from binding with the enzyme (Strelow et al., 2012. An example of noncompetitive inhibition is cyanide's effect on cytochrome C oxidase where the cyanide binds to the enzyme changing its conformation and preventing any further activity within the active site thus halting cellular metabolism (Leavesly et al., 2008). This is not to be confused with uncompetitive inhibition where the inhibitor binds

to an allosteric site while the substrate is in the active site preventing its dissociation. Most cases of uncompetitive inhibition are observed when the active site has multiple substrates enter the active site. Uncompetitive inhibition is characterized by a decrease in both V_{max} and K_m with a variable K_i value. A relevant example of uncompetitive inhibition is between acetaminophen and the COX2 enzyme. COX2 has two active sites. The first active site accepts and binds with arachidonic acid and the second binds with two oxygens. Acetaminophen's binding with COX2 prevents these two oxygens from leaving the active site and thus preventing the metabolism of arachidonic acid (Spence, 2022). Both noncompetitive inhibition and uncompetitive inhibition are forms of allosteric inhibition. Finally, there is partial inhibition where the inhibitor slows the function of the enzyme without preventing the enzyme from binding with the substrate (Strelow et al., 2012).

1.7 Microsomes and CYP (rk & rp)

Microsomes are small vesicles derived from the endoplasmic reticulum of cells that contain a variety of enzymes, many of which are cytochrome P450s (CYPs) (Palade, 1956). These enzymes primarily metabolize foreign organic compounds (El-Sherbeni, 2017). While the size of the microsomes often varies, the contents and their properties are often predictable. "Human liver microsomes provide the most convenient way to study CYP-mediated metabolism" (Jia, 2007). As a result, human liver microsomes are "the model of choice" for studying human drug metabolism because they contain the most relevant of the metabolizing enzymes in a simplified system as long as studies use a large pool from diverse individuals (Parmentier, 2007). Microsomes are much more convenient to use than liver cells.

The most relevant of the microsomal enzymes is the Cytochrome P450 (CYP) family. The CYP family is composed of 57 hemeprotein enzymes responsible for mainly metabolizing foreign organic and biotic chemicals (McDonnell and Dang, 2013; Sevrioukova and Poulos, 2013). This CYP family metabolizes foreign compounds by serving as catalysts in oxidation reactions between diatomic oxygen and the foreign compounds. The resulting products tend to be more water-soluble and therefore easier for the liver and urinary system to handle either by excretion or detoxification. The CYP enzymes tend to have similar structures but usually unique substrate specificity. However, the most prolific of these enzymes is CYP3A4. CYP3A4 belongs to the CYP3A family along with 3A43, 3A5 and 3A7 and it is considered the most important member of the family due to its sheer abundance as well as its broad metabolic promiscuity (Wright, 2019). CYP3A4 is responsible for about 50% of the metabolism of clinically prescribed drugs (de Wildt et al., 1999; Agrawal et al., 2010). CYP3A4 is also prone to cooperative substrate binding where more than one substrate binds to its active site (Sevrioukova and Poulos, 2013). This allosteric behavior is caused by the simultaneous binding of more than one substrate molecule in or near the active site. This also makes CYP3A4 somewhat unpredictable in its metabolism of xenobiotics as there are often other interactions between foreign compounds and the enzyme. Between its promiscuity and its unpredictable cooperative binding CYP3A4 is prone to undesirable drug-drug interactions and resulting toxicity such as the

aforementioned caffeine-caffeine oligomer that serves as an inhibitor of CYP3A4 (Sevrioukova and Poulos, 2013). For these reasons, CYP3A4 interactions between APAP and CAF with *A. annua* extracts are the focus of this study as they are common household drugs prone to drug-drug interactions.

Among the various molecules CYP3A4 interacts with is 7-benzoyloxy-4-trifluoromethyl coumarin (BFC), a pro-fluorescent molecule that, when oxidized by CYP3A4, yields a fluorescent product, at a rate that is linear with respect to BFC concentration up to 100 μM (Cheng and Guengerich, 2013). This interaction makes BFC ideal for use in assays that measure the activity of CYP3A4, as the degree to which a given solution fluoresces will be dependent on the degree to which a given molecule enhances or inhibits the activity of CYP3A4.

2.0 Hypothesis and Objectives

To determine CYP3A4 interactions between an herbal extract and a pure drug like APAP or CAF, a valid assay is needed. Prior studies used the Promega P-450 Glo assay specific for CYP3A4, but that proved quite costly, so this project aimed to validate the use of a more affordable assay using BFC.

2.1 Hypothesis (rp)

It was posited that the BFC assay would be a useful method whereby interactions can be measured between CAF and APAP and *A. annua* tea.

The null hypothesis is that the BFC assay will not provide a valid means to measure herbal extract interactions with pure drugs.

2.2 Objectives (rp)

1. Validate the efficacy of a BFC-based CYP3A4 assay using ketoconazole, a known inhibitor of CYP3A4.
2. Determine how *A. annua* tea interacts with BFC.
    2.1. Measure CYP3A4 activity in solutions with varying concentrations of *A. annua* tea to determine the IC_{50} of the tea using the BFC assay method.

3.0 Materials and Methods

3.1 Plant material and tea infusion preparation(rk)

The *Artemisia* tea was prepared as described by Kane et al (2022). Hot water extracts of *A. annua* were prepared using the following method: 2 g of dried leaves were boiled on a stir plate in 200 mL of water for 10 minutes, resulting in a concentration of 10 g/L. The tea was then filtered through a 2 mm stainless steel sieve, cooled, and sterile-filtered (0.22 μm), before being stored at −20℃.

3.2 Reagents (rk)

The human liver microsomes #H2620 (HLMs) were sourced from a 200-donor pool of males and females (Sekisui XenoTech, Kansas City, KS, USA) (Desrosiers et al., 2020) and diluted in a 250 mM sucrose solution #S-1888. BFC (7-benzyloxy-4-(trifluoromethyl)coumarin) #35721 was sourced from Cayman Chemical Company lot (Ann Arbor, Mi, USA). Ketoconazole #51212 was sourced from Cayman Chemical Company (Ann Arbor, Mi, USA). Potassium phosphate buffer was a 7.4 pH 0.1 M KPO_4 mixture of potassium phosphate dibasic from Fisher Bioreagents #BP363-500 (Pittsburgh, Pa, USA) and potassium phosphate monobasic #P5655 from Sigma Aldrich (St. Louis, MO, USA). Typically, this solution was made with 1.39 grams of potassium phosphate monobasic and 0.27 grams of potassium phosphate dibasic. Methanol was sourced from Fisher Chemical Thermo Fisher Scientific #203403 (Waltham, MA, USA). Tris buffer was 10 mM, with a pH of 8.0 created from 10 mM Tris HCl #T-3253, for a pH of 8.0, and was from Sigma Aldrich (St. Louis, MO, USA). If needed, the pH was adjusted to 8.0 with Trizma base #T1503-500G from Sigma Aldrich (St. Louis, MO, USA). The NADPH solution was mixed from the previously mentioned Tris buffer and NADPH tetrasodium salt #481973 sourced from EMG Millipore corp. (Darmstadt, Germany) to create a solution of 4 mM NADPH in 10 mM, pH 8 Tris buffer.

3.3 Ketoconazole IC_{50} determination via BFC assay (rk)

To determine the CYP450 3A4 IC_{50} for *A. annua* tea infusion, an assay using BFC as a fluorescent analyte and ketoconazole as an inhibitor was first used to validate the assay. Each trial was performed using a 96-well white assay plate (flat bottom polystyrene) #33-754 from Genesee Scientific and fluorescence read using the Victor Nivo plate reader with excitation at 435 nm and emission at 530 nm. The ketoconazole was dissolved in methanol at 1 μg/μL, from which 10 μL were removed and added to a 90 μL methanol solution and mixed before 10 μL were transferred to the next 90 μL of methanol. This continued three more times until the final dilution concentration of 1.88×10^{-4} mM was achieved. This experiment was repeated twice with each experiment containing three technical replicates which can be viewed in further detail in

Appendix A. The dilution concentrations, in µg/µL, were as follows: 0.00001, 0.0001, 0.001, 0.01, 0.1, and 1. Once the analytic wells received their respective masses of ketoconazole, the plate was incubated at 37°C for ten min to evaporate the methanol, followed by an aquarium air pump used to evaporate any remaining methanol. Each analytical well in the BFC assay contained 29 µL of 0.2 µg/µL HLM, 45 µL of 100 mM KPO_4 buffer (pH 7.4), and 1 µL of 5 mM BFC. Control wells containing no microsomes and no ketoconazole inhibitor were also done in triplicate. The microsome aliquot was replaced by 29 µL of a 250 mM sucrose solution; it was a microsome-free control. Following the addition of those reagents, the plate was incubated for 5 min at 37°C, before 25 µL of 4 mM NADPH in 10 mM Tris HCl was added to each well. The plate was incubated for an additional 30 min. Fluorescence was measured in the 96 well plate at a constant distance of 5 mm from the bottom of the plate. The no inhibitor control (NIC) wells were guidelines for the upper bounds of the fluorescence results and the no microsome (NMC) control fluorescence was subtracted from the fluorescence results:

$$Final\ Fluorescence = Recorded\ Fluorescence - NMC\ Fluorescence$$

Table 3: Concentrations of ketoconazole used in IC_{50} testing.

Ketoconazole (µg per 100 µL in well)	Ketoconazole (mM)
0.0001 µg/µL	0.000188
0.001 µg/µL	0.00188
0.01 µg/µL	0.0188
0.05 µg/µL	0.094
0.1 µg/µL	0.188
0.5 µg/µL	0.94
1 µg/µL	1.88
5 µg/µL	9.4
10 µg/µL	18.8
20 µg/µL	37.6

The data were analyzed using nonlinear regression analysis by GraphPad Prism 10 (San Diego, CA, USA) to provide an IC_{50} value that was used for further analysis. The data were not manipulated or normalized in any way as normalization would change the IC_{50} and there was no need for a background.

3.4 IC_{50} determination of *A. annua* tea (rk & rp)

To determine the IC_{50} concentration for artemisinin in *A. annua* DLA tea infusion the team adapted the previous MQP's process (Duncan & Togneri, 2023). The previous project used the Promega P450-Glo Assay specific to 3A4 to find their $IC_{50,}$ but we adjusted their process to be more consistent with our other BFC assays. The following serial dilutions were created with the tea and distilled water. This assay was repeated twice with technical triplicates and had the same assay reagent composition as the ketoconazole assay (Appendix A); however, the 45 µL of 100 mM KPO_4 buffer was replaced with 5 µL of 900 mM KPO_4 buffer and 40 µL of a given tea dilution. This allowed testing of higher tea concentrations with limited dilution. Serial tea dilutions were performed resulting in a concentration series from 580 µM to 0.563 µM. These dilutions were pipetted into wells of a Genesee Scientific 96-well plate corresponding to their concentration. Following that and the addition of 1 µL of 5 mM BFC and 29 µL of HLMs to each well, the plate was incubated at 37°C for 5 min, before being removed from the incubator and 25 µL of NADPH solution added per well. After that, the plate was returned to the incubator for 30 min, after which fluorescence was read using a Victor NIVO plate reader at Ex/Em 435/530 nm. The fluorescence derived from the plate was analyzed using a nonlinear regression analysis by GraphPad Prism 7 (San Diego, CA, USA) to provide an IC_{50} value that was available for further analysis.

Table 4: Concentrations of artemisinin used in IC_{50} testing.

Dilution Ratio	*A. annua* tea (µM tea artemisinin in well)
1	122.2
1:2	61.1
1:4	30.5
1:8	15.3
1:16	7.63
1:160	0.763
1:1600	0.0763
1:16000	0.00763
1:160000	0.000763

Most plant extracts have an innate fluorescence, so it was necessary to subtract the innate fluorescence of *A. annua* tea, to identify the actual fluorescence resulting from the BFC reaction. Two methods, ultimately, were used to accomplish this. In the differential method, a series of no

microsome controls (NMCs), repeating the concentrations of the tea, was added to the plate on the row below the corresponding experimental wells that contained microsomes. The fluorescence of the NMC wells was subtracted from the fluorescence of the experimental reaction (+HMC) wells:

Final Fluorescence = (+HMC Fluorescence) – (NMC Fluorescence)

The time based method subtracted the innate background fluorescence just prior to initiation of the reaction with NADPH, then NADPH was added and the plate incubated for 30 min after which the fluorescence was again read and recorded:

Final Fluorescence = Fluorescence at ~30 min post NADPH – Initial Fluorescence at -NADPH

4.0 Results (rp)

4.1 Ketoconazole IC_{50} Determination via BFC Assay (rp, rk's data)

Calculation of the IC_{50} of ketoconazole with respect to CYP3A4 was used to validate that the BFC method could be used to measure the necessary data for use in drug-herb interactions. The ketoconazole analyses are shown in Figure 6. This was repeated once more, and the average of the resulting values was taken to approximate the overall IC_{50} that was 7.01 ± 2.77 µM. For IC_{50} measurements the two values were reasonably replicated and are summarized in Table 5 along with an average of the two independent trials.

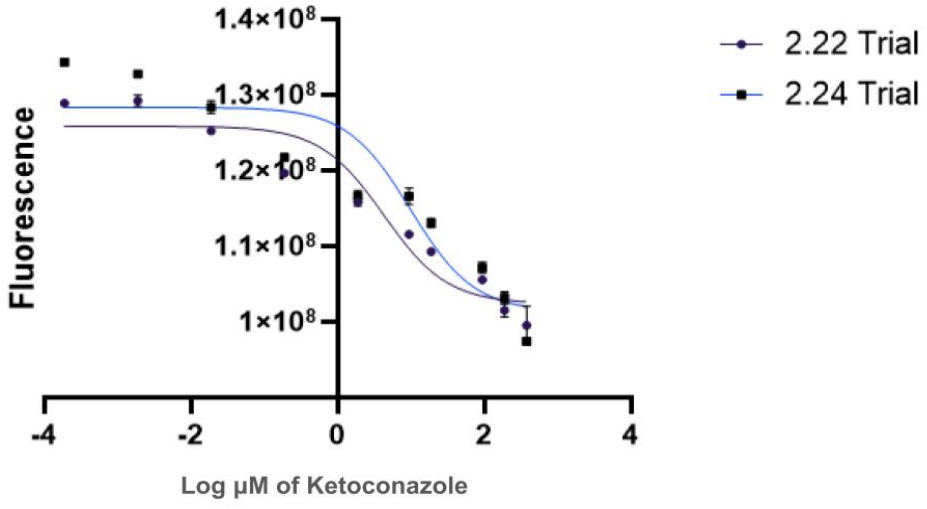

Figure 6: The overlaid ketoconazole inhibitory concentration curve had an averaged IC_{50} of 7.01 ± 2.77 µM. N=2 with each trial having 3 technical replicates. Bars represent Standard Error. (rk)

Table 5: IC_{50} values of the two triplicates, as calculated using AAT Bioquest's IC_{50} software, and the average of the two values.

Replicate	Ketoconazole IC_{50} Value (µM)
1	4.24
2	9.79
Average	7.01 ± 2.77

4.2 *A. annua* Tea Post-Incubation Reaction Experimentation (rp)

To determine the stability of the reaction before measuring the fluorescence in the plate reader we measured the fluorescence output at 4 and 35 min post incubation. This information allowed us to determine if there was a significant impact on the acquired fluorescence data. Thus, the plate was read as quickly as feasible after the completion of the incubation with NADPH, or within 4 minutes, and then 30 minutes later. Ultimately, it was determined that the error that would be generated by variance in the time to read the plate was not major (Figure 7).

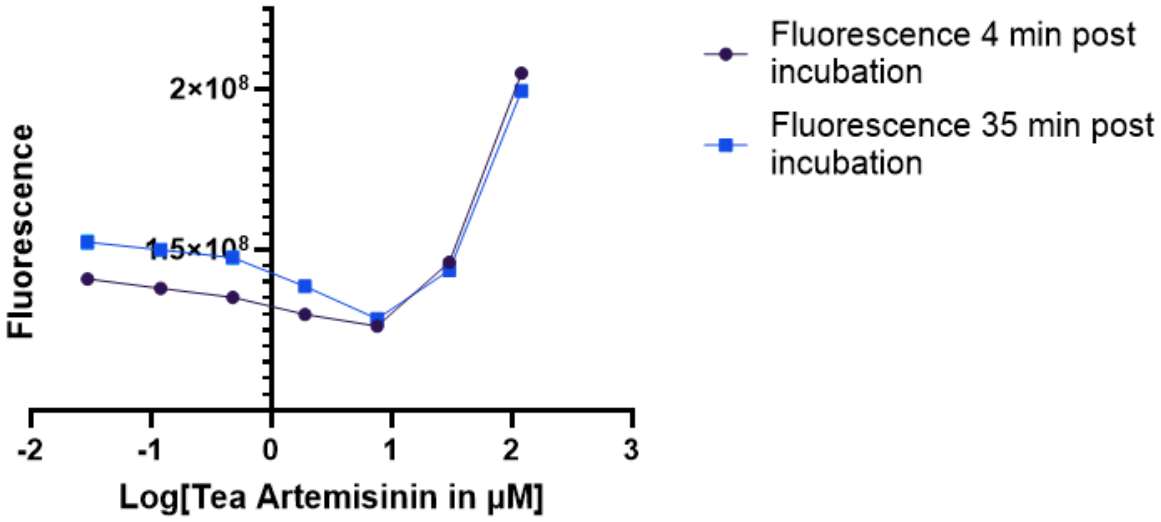

Figure 7: A dilution series comparing a 96-well plate incubated at 37°C for 30 minutes to a well incubated for 30 minutes then left at room temperature for 35 minutes. Standard error bars were included but they were too small to be seen without intense zooming. Calculated via Graph Pad Prism 10's software. (rk)

4.3 *A. annua* Tea IC_{50} Determination via BFC Assay (rp, rk's data)

Using the differential and time-based methods, we assessed which method would best account for the innate fluorescence in the *Artemisia* tea. Using the differential method, an IC_{50} of 1.95 µM was determined (Figure 8). Meanwhile, using the time-based method, an IC_{50} of 4.74 was measured (Figure 9). The IC_{50} values between the two methods used to account for the innate fluorescence of the *Artemisia* tea were not substantially different from one another. Because in the developing world *Artemisia* tea use is based on the amount of the plant's dried leaves used to brew the tea, the IC_{50} values in µg of dried plant leaves were also calculated from the artemisinin-based values and for the differential and time-based methods were, 2.5 and 6.08 µg, respectively (Table 6).

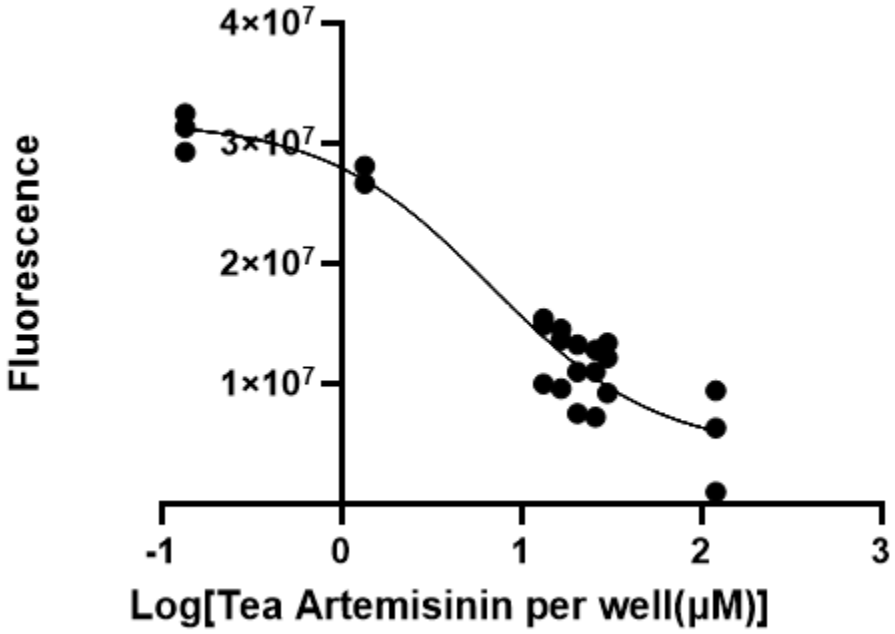

Figure 8: The results of the differential method for accounting for the innate *A. annua* fluorescence with an IC_{50} of 1.95 µM. Calculated via Graph Pad Prism 10's four parameter model. This experiment was done with three technical replicates. The above data show the three replicate data points at each concentration. (rk)

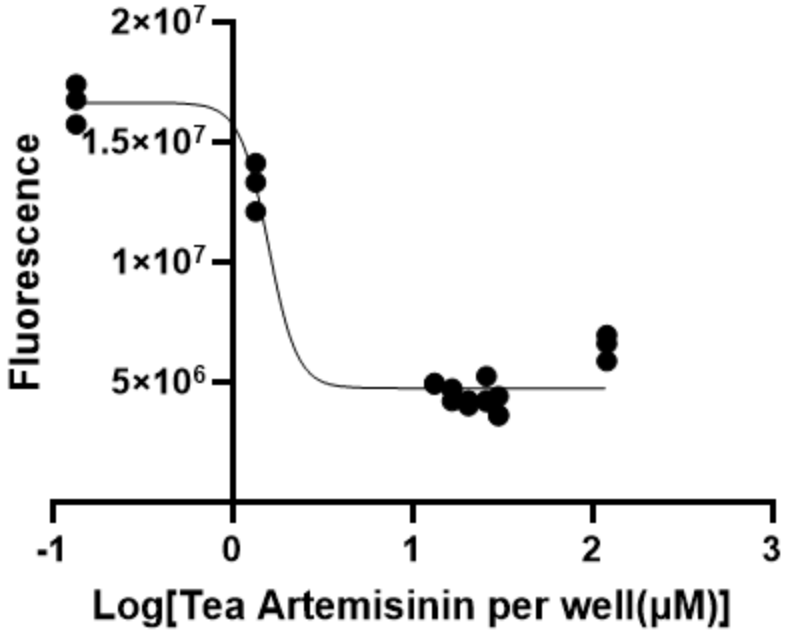

Figure 9: The results of the differential method for accounting for the innate *A. annua* fluorescence with an IC_{50} of 4.74 µM. Calculated via Graph Pad Prism 10's software. This experiment was done with three technical replicates. The above data show the three replicate data points at each concentration. (rk)

Table 6: IC_{50} values compared between two methods to account for the innate fluorescence of the tea extract. Methods 1 and 2 are differential and time-based methods, respectively.

Method	[Tea Artemisinin] IC_{50} Value (µM)	[*A. annua* tea dry weight equivalent] IC_{50} Value (µg)
1	1.95	2.5
2	4.74	6.08

5.0 Discussion and Conclusions (rk & rp)

The team sought a more affordable assay than the previously used P450-Glo CYP3A4 assay that was also convenient to use in a 96 well plate format for measuring hepatic CYP3A4 enzyme activity in liver microsomes (Duncan & Togneri, 2023). We thus focused on the suitability and usability of the fluorescent BFC-based CYP3A4 assay. While we found that this method was highly effective with pure drugs, e.g. ketoconazole, there were challenges when using plant extracts that are inherently fluorescent. When ketoconazole was used, an IC_{50} for CYP3A4 was determined to be 7.01 ± 2.77 μM, which correlated well with the range of values in the literature of 4.24 ± 2.83 μM to 1.75 ± 0.18 μM and well within 1 order of magnitude (Utkarsh et al., 2016; Cheng and Guengerich, 2013). Another study used a BFC assay and despite not using human liver microsomes had a similar CYP3A4 IC_{50} (Hansen et al. 2008). Furthermore, using the P450-Glo CYP 3A4 Desrosiers et al. (2020) measured an IC_{50} value of 5.67 μM for CYP3A4 in *A. annua* tea, which was close to what we measured using the BFC assay.

There are variations among different BFC protocols as noted in the literature. For example, we added NADPH, but many BFC-based fluorescence assays used NADPH-regeneration systems (Cheng and Guengerich, 2013). Indeed, nearly all the herb-CYP3A4 inhibition assays that could be found in the literature used an NADPH-generating system, which is more cost effective and produces a reliably consistent concentration of active NADPH, a molecule that is quite labile especially after long term storage. We also scaled down the quantity of each reagent proportionally so that the assay could be run in a 96-well plate. However, the largest issue of all was that there was fluorescence coming from the *A. annua* tea itself, which at high concentrations caused fluorescence values within unreacted tea to be almost 150% more than the fully reacted tea at the most dilute concentrations. Although this caused a lot of variance seen as noise in the higher concentration portions of our graphs, generally at or above 10 μM.

Another problematic issue was that the tea would regularly precipitate out a brown solid even when frozen, filter sterilized, and kept in a sterile environment. This precipitate seemed to be the result of freeze-thaw cycles and future work should all be done with tea from one consistent source, e.g., freshly made or all from the same thawed fraction. Otherwise there seemed to be unwanted scattering within trials that were dependent on how well mixed and how old the *A. annua tea* was, which proved challenging to standardize for experiments.

To address the issue of the innate fluorescence of *A. annua* tea, the team used two methods for dealing with it: subtraction of the fluorescence of reagents without microsomes, and subtraction of the fluorescence immediately after the addition of NADPH. The former method entailed creating another row of wells with equivalent concentrations of *A. annua* and equivalent concentrations, but without any microsomes, which is the source of the CYP3A4 enzyme. Instead of microsomes, their solvent, sucrose, was added in their stead. Essentially, the team made a series of no microsome controls. The fluorescence of these no microsome controls was subtracted from the fluorescence of the analytical wells.

The alternate method entailed taking fluorescence measurements just before adding the NADPH and then subtracting that from the fluorescence of the completed reaction. NADPH addition initiates the assay reaction and thus is a key point whereby one can account for all pre-reaction fluorescence.

To our knowledge there are no other studies that used the BFC assay to analyze the IC_{50} of a plant extract. Rather, most methods use various chromatography assays (Kondža et al., 2023; Georgiev et al., 2019; Sunaga et al., 2012; Yilue et al., 2019; Feltrin et al., 2020). However, we aimed for a faster assay that could be done in a 96-well plate similar to that used for the P450-Glo CYP3A4 assay previously used. While the P450-Glo CYP3A4 assay was highly effective with plant extracts (Ashour et al., 2019; Desrosiers et al., 2020), for an MQP the cost was prohibitive for obtaining adequate data to test a broader concentration series and drug-herb interactions.

6.0 Conclusions

As a result of the work that we conducted in this MQP, the BFC assay is suitable for use with both pure drugs and plant extracts, so long as one properly accounts for plant extract background fluorescence using either one of the methods described in this report.

7.0 References

Al-Dosari, Mohammed S., and Mohammad K. Parvez. 2018. "Novel Plant Inducers of PXR-Dependent Cytochrome P450 3A4 Expression in HepG2 Cells." *Saudi Pharmaceutical Journal* 26 (8): 1069–72. https://doi.org/10.1016/j.jsps.2018.05.016.

"Artemisia Annua: 6 Benefits, Dosage, & Safety | The Botanical Institute." 2022. September 6, 2022. https://botanicalinstitute.org/artemisia-annua/.

Ashour, Mohamed L, Fadia S Youssef, Haidy A Gad, and Michael Wink. 2017. "Inhibition of Cytochrome P450 (CYP3A4) Activity by Extracts from 57 Plants Used in Traditional Chinese Medicine (TCM)." *Pharmacognosy Magazine* 13 (50): 300–308. https://doi.org/10.4103/0973-1296.204561.

Bijnsdorp, Irene V., Elisa Giovannetti, and Godefridus J. Peters. 2011. "Analysis of Drug Interactions." In *Cancer Cell Culture: Methods and Protocols*, edited by Ian A. Cree, 421–34. Totowa, NJ: Humana Press. https://doi.org/10.1007/978-1-61779-080-5_34.

Cai, Tian-Yu, Yun-Rui Zhang, Jian-Bo Ji, and Jie Xing. 2017. "Investigation of the Component in Artemisia Annua L. Leading to Enhanced Antiplasmodial Potency of

Artemisinin via Regulation of Its Metabolism." *Journal of Ethnopharmacology* 207 (July): 86–91. https://doi.org/10.1016/j.jep.2017.06.025.

Cheng, Qian, and F. Peter. Guengerich. 2013. "High-Throughput Fluorescence Assay of Cytochrome P450 3A4." *Methods in Molecular Biology (Clifton, N.J.)* 987: 157–62. https://doi.org/10.1007/978-1-62703-321-3_14.

Cokol-Cakmak, Melike, Feray Bakan, Selim Cetiner, and Murat Cokol. 2018. "Diagonal Method to Measure Synergy Among Any Number of Drugs." *JoVE (Journal of Visualized Experiments)*, no. 136 (June): e57713. https://doi.org/10.3791/57713.

Cui, Liwang, and Xin-zhuan Su. 2009. "Discovery, Mechanisms of Action and Combination Therapy of Artemisinin." *Expert Review of Anti-Infective Therapy* 7 (8): 999–1013. https://doi.org/10.1586/eri.09.68.

Desrosiers, Matthew R., Alexis Mittelman, and Pamela J. Weathers. 2020. "Dried Leaf Artemisia Annua Improves Bioavailability of Artemisinin via Cytochrome P450 Inhibition and Enhances Artemisinin Efficacy Downstream." *Biomolecules* 10 (2): 254. https://doi.org/10.3390/biom10020254.

Duncan, H. and Sophia Togneri. 2023. Drug Herb Interactions: Artemisia Vs Artemisinin. : Worcester Polytechnic Institute.

Eatemadi, Ali, Hammed T. Aiyelabegan, Babak Negahdari, Mohammad Ali Mazlomi, Hadis Daraee, Nasim Daraee, Razieh Eatemadi, and Esmaeil Sadroddiny. 2017. "Role of Protease and Protease Inhibitors in Cancer Pathogenesis and Treatment." *Biomedicine & Pharmacotherapy* 86 (February): 221–31. https://doi.org/10.1016/j.biopha.2016.12.021.

Eagling, V. A., J. F. Tjia, and D. J. Back. 1998. "Differential Selectivity of Cytochrome P450 Inhibitors against Probe Substrates in Human and Rat Liver Microsomes." *British Journal of Clinical Pharmacology* 45 (2): 107–14. https://doi.org/10.1046/j.1365-2125.1998.00679.x.

El-Sherbeni, Ahmed A., and Ayman O. S. El-Kadi. 2017. "Microsomal Cytochrome P450 as a Target for Drug Discovery and Repurposing." *Drug Metabolism Reviews* 49 (1): 1–17. https://doi.org/10.1080/03602532.2016.1257021.

Elfawal, Mostafa A., Melissa J. Towler, Nicholas G. Reich, Pamela J. Weathers, and Stephen M. Rich. 2015. "Dried Whole-Plant Artemisia Annua Slows Evolution of Malaria Drug Resistance and Overcomes Resistance to Artemisinin." *Proceedings of the National Academy of Sciences of the United States of America* 112 (3): 821–26. https://doi.org/10.1073/pnas.1413127112.

Feltrin, Clarissa, Paula Freire Brambila, and Cláudia Maria Oliveira Simões. 2019. "Development of Caco-2 Cells-Based Gene Reporter Assays and Evaluation of Herb-Drug Interactions Involving CYP3A4 and CYP2D6 Gene Expression." *Chemico-Biological Interactions* 303 (April): 79–89. https://doi.org/10.1016/j.cbi.2019.01.030.

Feltrin, Clarissa, Ingrid Vicente Farias, Louis Pergaud Sandjo, Flávio Henrique Reginatto, and Cláudia Maria Oliveira Simões. 2020. "Effects of Standardized Medicinal Plant Extracts on Drug Metabolism Mediated by CYP3A4 and CYP2D6 Enzymes." *Chemical Research in Toxicology* 33 (9): 2408–19. https://doi.org/10.1021/acs.chemrestox.0c00182.

Foroozesh, Maryam, Jayalakshmi Sridhar, Navneet Goyal, and Jiawang Liu. 2019. "Coumarins and P450s, Studies Reported to-Date." *Molecules* 24 (8): 1620. https://doi.org/10.3390/molecules24081620.

Georgiev, Kaloyan D., Maya Radeva-Ilieva, Stanila Stoeva, and Iliya Zhelev. 2019. "Isolation, Analysis and in Vitro Assessment of CYP3A4 Inhibition by Methylxanthines Extracted from Pu-Erh and Bancha Tea Leaves." *Scientific Reports* 9 (1): 13941. https://doi.org/10.1038/s41598-019-50468-7.

Hazai, Eszter, László Vereczkey, and Katalin Monostory. 2002. "Reduction of Toxic Metabolite Formation of Acetaminophen." *Biochemical and Biophysical Research Communications* 291 (4): 1089–94. https://doi.org/10.1006/bbrc.2002.6541.

Hansen, Torstein Schrøder, and Odd Georg Nilsen. 2008. "In Vitro CYP3A4 Metabolism: Inhibition by Echinacea Purpurea and Choice of Substrate for the Evaluation of Herbal Inhibition." *Basic & Clinical Pharmacology & Toxicology* 103 (5): 445–49. https://doi.org/10.1111/j.1742-7843.2008.00307.x.

Hsu, Elisabeth. 2006. "The History of Qing Hao in the Chinese Materia Medica." *Transactions of the Royal Society of Tropical Medicine and Hygiene* 100 (6): 505–8. https://doi.org/10.1016/j.trstmh.2005.09.020.

Jia, Lee, and Xiaodong Liu. 2007. "The Conduct of Drug Metabolism Studies Considered Good Practice (II): In Vitro Experiments." *Current Drug Metabolism* 8 (8): 822–29. https://doi.org/10.2174/138920007782798207.

Jiang, Yiming, Xiaomei Fan, Ying Wang, Pan Chen, Hang Zeng, Huasen Tan, Frank J. Gonzalez, Min Huang, and Huichang Bi. 2015. "Schisandrol B Protects Against Acetaminophen-Induced Hepatotoxicity by Inhibition of CYP-Mediated Bioactivation and Regulation of Liver Regeneration." *Toxicological Sciences* 143 (1): 107–15. https://doi.org/10.1093/toxsci/kfu216.

Kane, Ndeye F., Bushra H. Kiani, Matthew R. Desrosiers, Melissa J. Towler, and Pamela J. Weathers. 2022. "Artemisia Extracts Differ from Artemisinin Effects on Human Hepatic CYP450s 2B6 and 3A4 in Vitro." *Journal of Ethnopharmacology* 298 (November): 115587. https://doi.org/10.1016/j.jep.2022.115587.

Kondža, Martin, Marta Mandić, Ivona Ivančić, Sanda Vladimir-Knežević, and Ivica Brizić. 2023. "Artemisia Annua L. Extracts Irreversibly Inhibit the Activity of CYP2B6 and CYP3A4 Enzymes." *Biomedicines* 11 (1): 232. https://doi.org/10.3390/biomedicines11010232.

Kostrubsky, Seva E., Jacqueline F. Sinclair, Stephen C. Strom, Sheryl Wood, Ellen Urda, Donna Beer Stolz, Yuan H. Wen, Shaila Kulkarni, and Abdul Mutlib. 2005. "Phenobarbital and Phenytoin Increased Acetaminophen Hepatotoxicity Due to Inhibition of UDP-Glucuronosyltransferases in Cultured Human Hepatocytes." *Toxicological Sciences: An Official Journal of the Society of Toxicology* 87 (1): 146–55. https://doi.org/10.1093/toxsci/kfi211.

Krenzelok, Edward P. 2009. "The FDA Acetaminophen Advisory Committee Meeting - What Is the Future of Acetaminophen in the United States? The Perspective of a Committee Member." *Clinical Toxicology (Philadelphia, Pa.)* 47 (8): 784–89. https://doi.org/10.1080/15563650903232345.

Larson, Erica C., Christopher D. Pond, Prem P. Rai, Teatulohi K. Matainaho, Pius Piskaut, Michael R. Franklin, and Louis R. Barrows. 2016. "Traditional Preparations and Methanol Extracts of Medicinal Plants from Papua New Guinea Exhibit Similar Cytochrome P450 Inhibition." *Evidence-Based Complementary and Alternative Medicine : eCAM* 2016: 7869710. https://doi.org/10.1155/2016/7869710.

Larson, Erica C., Laura B. Hathaway, John G. Lamb, Chris D. Pond, Prem P. Rai, Teatulohi K. Matainaho, Pius Piskaut, Louis R. Barrows, and Michael R. Franklin. "Interactions of Papua New Guinea Medicinal Plant Extracts with Antiretroviral Therapy." *Journal of Ethnopharmacology* 155, no. 3 (September 29, 2014): 1433–40. https://doi.org/10.1016/j.jep.2014.07.023.

Mazaleuskaya, Liudmila L., Katrin Sangkuhl, Caroline F. Thorn, Garret A. FitzGerald, Russ B. Altman, and Teri E. Klein. 2015. "PharmGKB Summary: Pathways of Acetaminophen Metabolism at the Therapeutic versus Toxic Doses." *Pharmacogenetics and Genomics* 25 (8): 416–26. https://doi.org/10.1097/FPC.0000000000000150.

Mazzari, Andre L. D. A., Flora Milton, Samantha Frangos, Ana C. B. Carvalho, Dâmaris Silveira, Francisco de Assis Rocha Neves, and Jose M. Prieto. 2016. "In Vitro Effects of Four Native Brazilian Medicinal Plants in CYP3A4 mRNA Gene Expression,

Glutathione Levels, and P-Glycoprotein Activity." *Frontiers in Pharmacology* 7 (August): 265. https://doi.org/10.3389/fphar.2016.00265.

McGill, Mitchell R., and Hartmut Jaeschke. 2013. "Metabolism and Disposition of Acetaminophen: Recent Advances in Relation to Hepatotoxicity and Diagnosis." *Pharmaceutical Research* 30 (9): 2174–87. https://doi.org/10.1007/s11095-013-1007-6.

Miller, Louis H., and Xinzhuan Su. 2011. "Artemisinin: Discovery from the Chinese Herbal Garden." *Cell* 146 (6): 855–58. https://doi.org/10.1016/j.cell.2011.08.024.

Nehlig, Astrid. 1999. "Are We Dependent upon Coffee and Caffeine? A Review on Human and Animal Data." *Neuroscience & Biobehavioral Reviews* 23 (4): 563–76. https://doi.org/10.1016/S0149-7634(98)00050-5.

Palade, G. E., and P. Siekevitz. 1956. "Liver Microsomes: An Integrated Morphological and Biochemical Study." *The Journal of Biophysical and Biochemical Cytology* 2 (2): 171–200.

Parmentier, Y., M.-J. Bossant, M. Bertrand, and B. Walther. 2007. "In Vitro Studies of Drug Metabolism." In , 231–57. Elsevier. https://doi.org/10.1016/B0-08-045044-X/00125-5.

PubChem. n.d.-a. "Acetaminophen." Accessed March 25, 2024. https://pubchem.ncbi.nlm.nih.gov/compound/1983.

———. n.d.-b. "Caffeine." Accessed March 25, 2024. https://pubchem.ncbi.nlm.nih.gov/compound/2519.

Septembre-Malaterre, Axelle, Mahary Lalarizo Rakoto, Claude Marodon, Yosra Bedoui, Jessica Nakab, Elisabeth Simon, Ludovic Hoarau, et al. 2020. "Artemisia Annua, a Traditional Plant Brought to Light." *International Journal of Molecular Sciences* 21 (14): 4986. https://doi.org/10.3390/ijms21144986.

Sevrioukova, Irina F. 2023. "Interaction of CYP3A4 with Caffeine: First Insights into Multiple Substrate Binding." *The Journal of Biological Chemistry* 299 (9): 105117. https://doi.org/10.1016/j.jbc.2023.105117.

Spence, J. David, Tilo Grosser, and Garret A. FitzGerald. 2022. "Acetaminophen, Nonsteroidal Anti-Inflammatory Drugs, and Hypertension." *Hypertension (Dallas, Tex.: 1979)* 79 (9): 1922–26. https://doi.org/10.1161/HYPERTENSIONAHA.122.19315.

Strelow, John, Walthere Dewe, Phillip W. Iversen, Harold B. Brooks, Jeffrey A. Radding, James McGee, and Jeffrey Weidner. 2012. "Mechanism of Action Assays for Enzymes." In *Assay Guidance Manual [Internet]*. Eli Lilly & Company and the National Center for Advancing Translational Sciences. https://www.ncbi.nlm.nih.gov/sites/books/NBK92001/.

Sunaga, Katsuyoshi, Kenichi Ohkawa, Kenichi Nakamura, Atsuko Ohkubo, Sonoko Harada, and Tadashi Tsuda. 2012. "Mechanism-Based Inhibition of Recombinant Human Cytochrome P450 3A4 by Tomato Juice Extract." *Biological and Pharmaceutical Bulletin* 35 (3): 329–34. https://doi.org/10.1248/bpb.35.329.

Temple, Jennifer L., Christophe Bernard, Steven E. Lipshultz, Jason D. Czachor, Joslyn A. Westphal, and Miriam A. Mestre. 2017. "The Safety of Ingested Caffeine: A Comprehensive Review." *Frontiers in Psychiatry* 8: 80. https://doi.org/10.3389/fpsyt.2017.00080.

World Health Organization, *The Use of non-pharmaceutical forms of artemisia*, (Geneva: WHO, 2019), https://www.who.int/news/item/10-10-2019-the-use-of-non-pharmaceutical-forms-of-artemisia.

Tu, Youyou. 2011. "The Discovery of Artemisinin (Qinghaosu) and Gifts from Chinese Medicine." *Nature Medicine* 17 (10): 1217–20. https://doi.org/10.1038/nm.2471.

Urry, Emily, Alexander Jetter, and Hans-Peter Landolt. 2016. "Assessment of CYP1A2 Enzyme Activity in Relation to Type-2 Diabetes and Habitual Caffeine Intake." *Nutrition & Metabolism* 13 (1): 66. https://doi.org/10.1186/s12986-016-0126-6.

Utkarsh, Doshi, Carol Loretz, and Albert P. Li. 2016. "In Vitro Evaluation of Hepatotoxic Drugs in Human Hepatocytes from Multiple Donors: Identification of P450 Activity as a Potential Risk Factor for Drug-Induced Liver Injuries." *Chemico-Biological Interactions*, Special Issue: Drug Induced Liver Injuries (DILI): Approaches to identify drugs with DILI potential, 255 (August): 12–22. https://doi.org/10.1016/j.cbi.2015.12.013.

Voet, Donald, Judith G. Voet, and Charlotte W. Pratt. 2016. *Fundamentals of Biochemistry: Life at the Molecular Level*. John Wiley & Sons.

Weathers, Pamela, Matthew Desrosiers, and Lucile Cornet-Vernet. 2023. "Chapter 1 Artemisia Annua, a Cost-Effective Sustainable Therapeutic for the Masses and the Political Challenges for Its Implementation." In *Chapter 1 Artemisia Annua, a Cost-Effective Sustainable Therapeutic for the Masses and the Political Challenges for Its Implementation*, 21–36. De Gruyter. https://doi.org/10.1515/9783110757507-002.

Weathers, Pamela J. 2023. "Artemisinin as a Therapeutic vs. Its More Complex Artemisia Source Material." *Natural Product Reports* 40 (7): 1158–69. https://doi.org/10.1039/d2np00072e.

Whirl-Carrillo, Michelle, Rachel Huddart, Li Gong, Katrin Sangkuhl, Caroline F. Thorn, Ryan Whaley, and Teri E. Klein. 2021. "An Evidence-Based Framework for Evaluating

Pharmacogenomics Knowledge for Personalized Medicine." *Clinical Pharmacology and Therapeutics* 110 (3): 563–72. https://doi.org/10.1002/cpt.2350.

Willson, Cyril. 2018. "The Clinical Toxicology of Caffeine: A Review and Case Study." *Toxicology Reports* 5 (November): 1140–52. https://doi.org/10.1016/j.toxrep.2018.11.002.

Wright, William C., Jude Chenge, and Taosheng Chen. 2019. "Structural Perspectives of the CYP3A Family and Their Small Molecule Modulators in Drug Metabolism." *Liver Research* 3 (3–4): 132–42. https://doi.org/10.1016/j.livres.2019.08.001.

Zhang, Yilue, Thankhoe A. Rants'o, Da Jung, Elizabeth Lopez, Kodye Abbott, Satyanarayana R. Pondugula, Lane McLendon, Jingjing Qian, Richard A. Hansen, and Angela I. Calderón. 2019. "Screening for CYP3A4 Inhibition and Induction Coupled to Parallel Artificial Membrane Permeability Assay (PAMPA) for Prediction of Botanical-Drug Interactions: The Case of Açaí and Maca." *Phytomedicine* 59 (June): 152915. https://doi.org/10.1016/j.phymed.2019.152915.

Appendix A — SOP BFC Assay Ketoconazole IC50 Determination (rk)

BFC Assay

Reagents:

1. Ketoconazole: from Cayman Chemical Company #51212
2. Methanol: from Fisher Chemical Thermo Fisher Scientific #203403
3. 100 mM BFC solution: dissolved in DMSO Cayman Chemical Company #3572
4. 7.4 pH KPO_4 Buffer 0.1 M created with both potassium phosphate dibasic (BP363-500) and potassium phosphate monobasic anhydrous both sourced from Fisher Bioreagents.
5. Sucrose solution: 250 mM diluted in water and sourced from Sigma Aldrich
6. Distilled water
7. Human Liver Microsomes: sourced from Sekisui XenoTech #H2620 with a protein content of 20 mg/ml and a P450 content of 335 pmol/mg diluted with 250 mM sucrose #S-1888 to 0.2 µg/µL.
8. NADPH: 4 mM in NADPH in pH 8 10 mM Tris HCl
9. Tris buffer: 10 mM of Tris HCl #T-3253 from Sigma Aldrich diluted in water. The pH was adjusted to 8.0 with Trizma base #T1503-500G from Sigma Aldrich.

Tools:

1. 96-well white assay plate (flat bottom polystyrene) #33-754 from Genesee Scientific
2. Incubator set to 37°C
3. 1000, 200, 100, 20, and 2 µL micropipettes
4. Victor Nivo Plate Reader
5. Aquarium Air Pump

Procedure:

1. Removed KPO_4 from the 4°C refrigerator to warm to room temperature.
2. Dissolved ketoconazole in corresponding µLs methanol and pipetted it into the wells of a 96 well 300 µL white assay plate.
    a. Refer to the table below for amounts.
    b. The 96-well plate was placed into the 37°C incubator to evaporate the methanol.
3. The remaining methanol was evaporated using the air pump.
4. Human liver microsome (HLM) aliquots of 0.2 µg/µL are removed from the -20 freezer°C.
5. A master solution of 1 µL 100 mM BFC was diluted in 19 µL water for each well used. Then 45 µL of KPO_4 and 29 µL of HLM was added for each well used. The master solution was mixed by pipetting. 75 µL of mixture was pipetted into each well.

    a. There were typically 27 wells so a solution of 2.3 µL BFC was mixed with 43.9 µL of water
    b. One column received no inhibitor but had all of these reagents added via the master mixture.
6. The NMC was prepared separately with these three wells receiving 29 µL of sucrose, 45 µL of KPO_4 and 1 µL of the diluted BFC (and no ketoconazole) to create No Microsome Control (NMC).
7. The plate was then pre-incubated at 37°C for 5 minutes.
8. 25 µL of 4 mM NADPH (in 10 mM Tris buffer at pH 8) is added to each well by a multi-channel pipette to start the reaction.
9. The wells were then incubated at 37°C for 30 minutes.
10. The plate's fluorescence was then read by the Victor NIVO plate reader on another floor. The fluorescence of the analytical wells was prepared for analysis by subtracting the average fluorescence of the wells with the highest inhibitor concentration from the well being analyzed. While the NIC wells were supposed to account for all background fluorescence, the fluorescence of the lowest inhibitor concentration wells was still sometimes higher. For example, the raw A3 fluorescence - average column 11 fluorescence = adjusted A3 fluorescence.

Table 6: Table showing the contents of each well within a 96 well plate. Rows 2-11 are analytical wells. Columns 1 and 2 contain NMC's and NIC's for further calculations and calibrations.

Amount of Keto	NMC	NIC	0.0001 µg	0.001 µg	0.01 µg	0.05 µg	0.1 µg	0.5 µg	1 µg	5 µg	10 µg	20 µg
	1	2	3	3	4	5	6	7	8	9	10	11
A	1 µL BFC, 29 µL Sucrose, 45 µL KPO_4, 25µL NADPH	1 µL BFC, 29 µL HLM, 45 µL KPO_4, 25µL NADPH	1 µL BFC, 29 µL HLM, 45 µL KPO_4, 25µL NADPH	1 µL BFC, 29 µL HLM, 45 µL KPO_4, 25µL NADPH	1 µL BFC, 29 µL HLM, 45 µL KPO_4, 25µL NADPH	1 µL BFC, 29 µL HLM, 45 µL KPO_4, 25µL NADPH	1 µL BFC, 29 µL HLM, 45 µL KPO_4, 25µL NADPH	1 µL BFC, 29 µL HLM, 45 µL KPO_4, 25µL NADPH	1 µL BFC, 29 µL HLM, 45 µL KPO_4, 25µL NADPH	1 µL BFC, 29 µL HLM, 45 µL KPO_4, 25µL NADPH	1 µL BFC, 29 µL HLM, 45 µL KPO_4, 25µL NADPH	1 µL BFC, 29 µL HLM, 45 µL KPO_4, 25µL NADPH
B	1 µL BFC, 29 µL Sucrose, 45 µL KPO_4, 25µL NADPH	1 µL BFC, 29 µL HLM, 45 µL KPO_4, 25µL NADPH	1 µL BFC, 29 µL HLM, 45 µL KPO_4, 25µL NADPH	1 µL BFC, 29 µL HLM, 45 µL KPO_4, 25µL NADPH	1 µL BFC, 29 µL HLM, 45 µL KPO_4, 25µL NADPH	1 µL BFC, 29 µL HLM, 45 µL KPO_4, 25µL NADPH	1 µL BFC, 29 µL HLM, 45 µL KPO_4, 25µL NADPH	1 µL BFC, 29 µL HLM, 45 µL KPO_4, 25µL NADPH	1 µL BFC, 29 µL HLM, 45 µL KPO_4, 25µL NADPH	1 µL BFC, 29 µL HLM, 45 µL KPO_4, 25µL NADPH	1 µL BFC, 29 µL HLM, 45 µL KPO_4, 25µL NADPH	1 µL BFC, 29 µL HLM, 45 µL KPO_4, 25µL NADPH
C	1 µL BFC, 29 µL Sucrose, 45 µL KPO_4, 25µL NADPH	1 µL BFC, 29 µL HLM, 45 µL KPO_4, 25µL NADPH	1 µL BFC, 29 µL HLM, 45 µL KPO_4, 25µL NADPH	1 µL BFC, 29 µL HLM, 45 µL KPO_4, 25µL NADPH	1 µL BFC, 29 µL HLM, 45 µL KPO_4, 25µL NADPH	1 µL BFC, 29 µL HLM, 45 µL KPO_4, 25µL NADPH	1 µL BFC, 29 µL HLM, 45 µL KPO_4, 25µL NADPH	1 µL BFC, 29 µL HLM, 45 µL KPO_4, 25µL NADPH	1 µL BFC, 29 µL HLM, 45 µL KPO_4, 25µL NADPH	1 µL BFC, 29 µL HLM, 45 µL KPO_4, 25µL NADPH	1 µL BFC, 29 µL HLM, 45 µL KPO_4, 25µL NADPH	1 µL BFC, 29 µL HLM, 45 µL KPO_4, 25µL NADPH
Final Concentrations	.5 µM BFC, 72.5 mM sucrose, 45 mM, KPO_4, 1mM NADPH	.5 µM BFC, 72.5 mM sucrose, 45 mM, KPO_4, 1mM NADPH	.5 µM BFC, 72.5 mM sucrose, 45 mM, KPO_4, 1mM NADPH	.5 µM BFC, 72.5 mM sucrose, 45 mM, KPO_4, 1mM NADPH 0.00188 µM Keto	.5 µM BFC, 72.5 mM sucrose, 45 mM, KPO_4, 1mM NADPH 0.0188 µM Keto	.5 µM BFC, 72.5 mM sucrose, 45 mM, KPO_4, 1mM NADPH 0.094 µM Keto	.5 µM BFC, 72.5 mM sucrose, 45 mM, KPO_4, 1mM NADPH 0.188 µM Keto	.5 µM BFC, 72.5 mM sucrose, 45 mM, KPO_4, 1mM NADPH 0.94 µM Keto	.5 µM BFC, 72.5 mM sucrose, 45 mM, KPO_4, 1mM NADPH 1.88 µM Keto	.5 µM BFC, 72.5 mM sucrose, 45 mM, KPO_4, 1mM NADPH 9.4 µM Keto	.5 µM BFC, 72.5 mM sucrose, 45 mM, KPO_4, 1mM NADPH 18.8 µM Keto	.5 µM BFC, 72.5 mM sucrose, 45 mM, KPO_4, 1mM NADPH, 37.6 µM Keto

Appendix B — SOP BFC Assay Caffeine IC50 Determination (rk)

BFC Assay

Reagents:

1. 4.48 M Caffeine: from Sigma Aldrich #C0750
2. Ketoconazole: from Cayman Chemical Company #51212
3. Methanol: from Fisher Chemical Thermo Fisher Scientific #203403
4. 100 mM BFC solution: dissolved in DMSO Cayman Chemical Company #3572
5. 7.4 pH KPO_4 Buffer 0.9 M created with both potassium phosphate dibasic (BP363-500) and potassium phosphate monobasic anhydrous both sourced from Fisher Bioreagents.
6. Sucrose solution: 250 mM diluted in water and sourced from Sigma Aldrich
7. Distilled water
8. Human Liver Microsomes: sourced from Sekisui XenoTech #H2620 with a protein content of 20 mg/ml and a P450 content of 335 pmol/mg diluted with 250 mM sucrose #S-1888 to 0.2 µg/µL.
9. NADPH: 4 mM in NADPH in pH 8 10 mM Tris HCl
10. Tris buffer: 10 mM of Tris HCl #T-3253 from Sigma Aldrich diluted in water. The pH was adjusted to 8.0 with Trizma base #T1503-500G from Sigma Aldrich.

Tools:

1. 96-well white assay plate (flat bottom polystyrene) #33-754 from Genesee Scientific
2. Incubator set to 37°C
3. 1000, 200, 100, 20, and 2 µL micropipettes
4. Victor Nivo Plate Reader
5. Aquarium Air Pump

Procedure:

1. Removed KPO_4 from the 4°C refrigerator to warm to room temperature.
2. Dissolved ketoconazole in corresponding µLs methanol and pipetted it into the wells of a 96 well 300 µL white assay plate.
    a. Refer to the table below for amounts.
    b. The 96-well plate was placed into the 37°C incubator to evaporate the methanol.
3. The remaining methanol was evaporated using the air pump.
4. Human liver microsome (HLM) aliquots of 0.2 µg/µL are removed from the -20 freezer°C.
5. A master solution of 1 µL 100 mM BFC was diluted in 19 µL water for each well used. Then 5 µL of KPO_4 and 29 µL of HLM was added for each well used. The master solution was mixed by pipetting. 75 µL of mixture was pipetted into each well.

c. There were typically 27 wells so a solution of 2.3 µL BFC was mixed with 43.9 µL of water
d. One column received no inhibitor but had all of these reagents added via the master mixture.

6. The NMC was prepared separately with these three wells receiving 29 µL of sucrose, 45 µL of KPO_4 and 1 µL of the diluted BFC (and no ketoconazole) to create No Microsome Control (NMC).
7. The plate was then pre-incubated at 37°C for 5 minutes.
8. 25 µL of 4 mM NADPH (in 10 mM Tris buffer at pH 8) is added to each well by a multi-channel pipette to start the reaction.
9. The wells were then incubated at 37°C for 30 minutes.
10. The plate's fluorescence was then read by the Victor NIVO plate reader on another floor. The fluorescence of the analytical wells was prepared for analysis by subtracting the average fluorescence of the wells with the highest inhibitor concentration from the well being analyzed. While the NIC wells were supposed to account for all background fluorescence, the fluorescence of the lowest inhibitor concentration wells was still sometimes higher. For example, the raw A3 fluorescence - average column 11 fluorescence = adjusted A3 fluorescence.

Table 7: Table showing the contents of each well within a 96 well plate. Rows 4-11 are analytical wells. Columns 1 -3 contain NMC’s and NIC’s for further calculations and calibrations and a ketoconazole well for control.

Amount of Caffeine	Keto (0.5 µg per well)	NMC	NIC	0.0448 µM CAF	0.448 µM CAF	4.48 µM CAF	44.8 µM CAF	448 µM CAF	4480 µM CAF	0.00448 M CAF	0.0448 M CAF	0.448 M CAF	4.48 M CAF
	1	2	3	4	5	5	6	7	8	9	10	11	12
A	1 µL BFC, 29 µL HLM, 5 µL KPO_4, 25µL NADPH	1 µL BFC, 29 µL Sucrose, 5 µL KPO_4, 25µL NADPH	1 µL BFC, 29 µL HLM, 5 µL KPO_4, 25µL NADPH	1 µL BFC, 29 µL HLM, 5 µL KPO_4, 25µL NADPH	1 µL BFC, 29 µL HLM, 5 µL KPO_4, 25µL NADPH	1 µL BFC, 29 µL HLM, 5 µL KPO_4, 25µL NADPH	1 µL BFC, 29 µL HLM, 5 µL KPO_4, 25µL NADPH	1 µL BFC, 29 µL HLM, 5 µL KPO_4, 25µL NADPH	1 µL BFC, 29 µL HLM, 5 µL KPO_4, 25µL NADPH	1 µL BFC, 29 µL HLM, 5 µL KPO_4, 25µL NADPH	1 µL BFC, 29 µL HLM, 5 µL KPO_4, 25µL NADPH	1 µL BFC, 29 µL HLM, 5 µL KPO_4, 25µL NADPH	1 µL BFC, 29 µL HLM, 5 µL KPO_4, 25µL NADPH
B	1 µL BFC, 29 µL HLM, 5 µL KPO_4, 25µL NADPH	1 µL BFC, 29 µL Sucrose, 5 µL KPO_4, 25µL NADPH	1 µL BFC, 29 µL HLM, 5 µL KPO_4, 25µL NADPH	1 µL BFC, 29 µL HLM, 5 µL KPO_4, 25µL NADPH	1 µL BFC, 29 µL HLM, 5 µL KPO_4, 25µL NADPH	1 µL BFC, 29 µL HLM, 5 µL KPO_4, 25µL NADPH	1 µL BFC, 29 µL HLM, 5 µL KPO_4, 25µL NADPH	1 µL BFC, 29 µL HLM, 5 µL KPO_4, 25µL NADPH	1 µL BFC, 29 µL HLM, 5 µL KPO_4, 25µL NADPH	1 µL BFC, 29 µL HLM, 5 µL KPO_4, 25µL NADPH	1 µL BFC, 29 µL HLM, 5 µL KPO_4, 25µL NADPH	1 µL BFC, 29 µL HLM, 5 µL KPO_4, 25µL NADPH	1 µL BFC, 29 µL HLM, 5 µL KPO_4, 25µL NADPH
C	1 µL BFC, 29 µL HLM, 5 µL KPO_4, 25µL NADPH	1 µL BFC, 29 µL Sucrose, 5 µL KPO_4, 25µL NADPH	1 µL BFC, 29 µL HLM, 5 µL KPO_4, 25µL NADPH	1 µL BFC, 29 µL HLM, 5 µL KPO_4, 25µL NADPH	1 µL BFC, 29 µL HLM, 5 µL KPO_4, 25µL NADPH	1 µL BFC, 29 µL HLM, 5 µL KPO_4, 25µL NADPH	1 µL BFC, 29 µL HLM, 5 µL KPO_4, 25µL NADPH	1 µL BFC, 29 µL HLM, 5 µL KPO_4, 25µL NADPH	1 µL BFC, 29 µL HLM, 5 µL KPO_4, 25µL NADPH	1 µL BFC, 29 µL HLM, 5 µL KPO_4, 25µL NADPH	1 µL BFC, 29 µL HLM, 5 µL KPO_4, 25µL NADPH	1 µL BFC, 29 µL HLM, 5 µL KPO_4, 25µL NADPH	1 µL BFC, 29 µL HLM, 5 µL KPO_4, 25µL NADPH
Final Concentrations	1 µL BFC, 29 µL HLM, 5 µL KPO_4, 25µL NADPH, 0.094 µM Keto	.5 µM BFC, 72.5 mM sucrose, 45 mM, KPO_4, 1mM NADPH	.5 µM BFC, 72.5 mM sucrose, 45 mM, KPO_4, 1mM NADPH	.5 µM BFC, 72.5 mM sucrose, 45 mM, KPO_4, 1mM NADPH, 0.0448 µM CAF	.5 µM BFC, 72.5 mM sucrose, 45 mM, KPO_4, 1mM NADPH 0.448 µM CAF	.5 µM BFC, 72.5 mM sucrose, 45 mM, KPO_4, 1mM NADPH 4.48 µM CAF	.5 µM BFC, 72.5 mM sucrose, 45 mM, KPO_4, 1mM NADPH 44.8 µM CAF	.5 µM BFC, 72.5 mM sucrose, 45 mM, KPO_4, 1mM NADPH 448 µM CAF	.5 µM BFC, 72.5 mM sucrose, 45 mM, KPO_4, 1mM NADPH 4480 µM CAF	.5 µM BFC, 72.5 mM sucrose, 45 mM, KPO_4, 1mM NADPH 0.00448 M CAF	.5 µM BFC, 72.5 mM sucrose, 45 mM, KPO_4, 1mM NADPH 0.0448 M CAF	.5 µM BFC, 72.5 mM sucrose, 45 mM, KPO_4, 1mM NADPH 0.448µM CAF	.5 µM BFC, 72.5 mM sucrose, 45 mM, KPO_4, 1mM NADPH, 4.48 M CAF

Appendix C — SOP BFC Assay Acetaminophen IC50 Determination (rk)

1. 3.84 mM acetaminophen from Thermo Fisher Scientific #102330050
2. Ketoconazole: from Cayman Chemical Company #51212
3. Methanol: from Fisher Chemical Thermo Fisher Scientific #203403
4. 100 mM BFC solution: dissolved in DMSO Cayman Chemical Company #3572
5. 7.4 pH KPO_4 Buffer 0.9 M created with both potassium phosphate dibasic (BP363-500) and potassium phosphate monobasic anhydrous both sourced from Fisher Bioreagents.
6. Sucrose solution: 250 mM diluted in water and sourced from Sigma Aldrich
7. Distilled water
8. Human Liver Microsomes: sourced from Sekisui XenoTech #H2620 with a protein content of 20 mg/ml and a P450 content of 335 pmol/mg diluted with 250 mM sucrose #S-1888 to 0.2 µg/µL.
9. NADPH: 4 mM in NADPH in pH 8 10 mM Tris HCl
10. Tris buffer: 10 mM of Tris HCl #T-3253 from Sigma Aldrich diluted in water. The pH was adjusted to 8.0 with Trizma base #T1503-500G from Sigma Aldrich.

Tools:

1. 96-well white assay plate (flat bottom polystyrene) #33-754 from Genesee Scientific
2. Incubator set to 37°C
3. 1000, 200, 100, 20, and 2 µL micropipettes
4. Victor Nivo Plate Reader
5. Aquarium Air Pump

Procedure:

1. Removed KPO_4 from the 4°C refrigerator to warm to room temperature.
2. Dissolved ketoconazole in corresponding µLs methanol and pipetted it into the wells of a 96 well 300 µL white assay plate.
    a. Refer to the table below for amounts.
    b. The 96-well plate was placed into the 37°C incubator to evaporate the methanol.
3. The remaining methanol was evaporated using the air pump.
4. Human liver microsome (HLM) aliquots of 0.2 µg/µL are removed from the -20 freezer°C.
5. A master solution of 1 µL 100 mM BFC was diluted in 19 µL water for each well used. Then 5 µL of KPO_4 and 29 µL of HLM was added for each well used. The master solution was mixed by pipetting. 75 µL of mixture was pipetted into each well.
    e. There were typically 27 wells so a solution of 2.3 µL BFC was mixed with 43.9 µL of water

f. One column received no inhibitor but had all of these reagents added via the master mixture.

6. The NMC was prepared separately with these three wells receiving 29 µL of sucrose, 45 µL of KPO_4 and 1 µL of the diluted BFC (and no ketoconazole) to create No Microsome Control (NMC).
7. The plate was then pre-incubated at 37°C for 5 minutes.
8. 25 µL of 4 mM NADPH (in 10 mM Tris buffer at pH 8) is added to each well by a multi-channel pipette to start the reaction.
9. The wells were then incubated at 37°C for 30 minutes.
10. The plate's fluorescence was then read by the Victor NIVO plate reader on another floor. The fluorescence of the analytical wells was prepared for analysis by subtracting the average fluorescence of the wells with the highest inhibitor concentration from the well being analyzed. While the NIC wells were supposed to account for all background fluorescence, the fluorescence of the lowest inhibitor concentration wells was still sometimes higher. For example, the raw A3 fluorescence - average column 11 fluorescence = adjusted A3 fluorescence.

Table 8: Table showing the contents of each well within a 96 well plate. Rows 4-11 are analytical wells. Columns 1 -3 contain NMC's and NIC's for further calculations and calibrations and a ketoconazole well for control.

Amount of APAP	Keto (0.5 µg per well)	NMC	NIC	1.9 µM	3.9 µM	7.81 µM	15.625 µM	31.25 µM	62.5 µM	62.5 µM	125 µM	0.384 mM	3.84mM
	1	1	2	3	3	4	5	6	7	8	9	10	11
A	1 µL BFC, 29 µL HLM, 5 µL KPO_4, 25µL NADPH	1 µL BFC, 29 µL Sucrose, 5 µL KPO_4, 25µL NADPH	1 µL BFC, 29 µL HLM, 5 µL KPO_4, 25µL NADPH	1 µL BFC, 29 µL HLM, 5 µL KPO_4, 25µL NADPH	1 µL BFC, 29 µL HLM, 5 µL KPO_4, 25µL NADPH	1 µL BFC, 29 µL HLM, 5 µL KPO_4, 25µL NADPH	1 µL BFC, 29 µL HLM, 5 µL KPO_4, 25µL NADPH	1 µL BFC, 29 µL HLM, 5 µL KPO_4, 25µL NADPH	1 µL BFC, 29 µL HLM, 5 µL KPO_4, 25µL NADPH	1 µL BFC, 29 µL HLM, 5 µL KPO_4, 25µL NADPH	1 µL BFC, 29 µL HLM, 5 µL KPO_4, 25µL NADPH	1 µL BFC, 29 µL HLM, 5 µL KPO_4, 25µL NADPH	1 µL BFC, 29 µL HLM, 5 µL KPO_4, 25µL NADPH
B	1 µL BFC, 29 µL HLM, 5 µL KPO_4, 25µL NADPH	1 µL BFC, 29 µL Sucrose, 5 µL KPO_4, 25µL NADPH	1 µL BFC, 29 µL HLM, 5 µL KPO_4, 25µL NADPH	1 µL BFC, 29 µL HLM, 5 µL KPO_4, 25µL NADPH	1 µL BFC, 29 µL HLM, 5 µL KPO_4, 25µL NADPH	1 µL BFC, 29 µL HLM, 5 µL KPO_4, 25µL NADPH	1 µL BFC, 29 µL HLM, 5 µL KPO_4, 25µL NADPH	1 µL BFC, 29 µL HLM, 5 µL KPO_4, 25µL NADPH	1 µL BFC, 29 µL HLM, 5 µL KPO_4, 25µL NADPH	1 µL BFC, 29 µL HLM, 5 µL KPO_4, 25µL NADPH	1 µL BFC, 29 µL HLM, 5 µL KPO_4, 25µL NADPH	1 µL BFC, 29 µL HLM, 5 µL KPO_4, 25µL NADPH	1 µL BFC, 29 µL HLM, 5 µL KPO_4, 25µL NADPH
C	1 µL BFC, 29 µL HLM, 5 µL KPO_4, 25µL NADPH	1 µL BFC, 29 µL Sucrose, 5 µL KPO_4, 25µL NADPH	1 µL BFC, 29 µL HLM, 5 µL KPO_4, 25µL NADPH	1 µL BFC, 29 µL HLM, 5 µL KPO_4, 25µL NADPH	1 µL BFC, 29 µL HLM, 5 µL KPO_4, 25µL NADPH	1 µL BFC, 29 µL HLM, 5 µL KPO_4, 25µL NADPH	1 µL BFC, 29 µL HLM, 5 µL KPO_4, 25µL NADPH	1 µL BFC, 29 µL HLM, 5 µL KPO_4, 25µL NADPH	1 µL BFC, 29 µL HLM, 5 µL KPO_4, 25µL NADPH	1 µL BFC, 29 µL HLM, 5 µL KPO_4, 25µL NADPH	1 µL BFC, 29 µL HLM, 5 µL KPO_4, 25µL NADPH	1 µL BFC, 29 µL HLM, 5 µL KPO_4, 25µL NADPH	1 µL BFC, 29 µL HLM, 5 µL KPO_4, 25µL NADPH
Final Concentrations	1 µL BFC, 29 µL HLM, 5 µL KPO_4, 25µL NADPH, 0.094 µM Keto	.5 µM BFC, 72.5 mM sucrose, 45 mM, KPO_4, 1mM NADPH	.5 µM BFC, 72.5 mM sucrose, 45 mM, KPO_4, 1mM NADPH	.5 µM BFC, 72.5 mM sucrose, 45 mM, KPO_4, 1mM NADPH	.5 µM BFC, 72.5 mM sucrose, 45 mM, KPO_4, 1mM NADPH 3.84 µM APAP	.5 µM BFC, 72.5 mM sucrose, 45 mM, KPO_4, 1mM NADPH 38.4 µM APAP	.5 µM BFC, 72.5 mM sucrose, 45 mM, KPO_4, 1mM NADPH 384 µM APAP	.5 µM BFC, 72.5 mM sucrose, 45 mM, KPO_4, 1mM NADPH 3.84mM APAP	.5 µM BFC, 72.5 mM sucrose, 45 mM, KPO_4, 1mM NADP0 .384 mM	.5 µM BFC, 72.5 mM sucrose, 45 mM, KPO_4, 1mM NADPH 3.84 mM	.5 µM BFC, 72.5 mM sucrose, 45 mM, KPO_4, 1mM NADPH 38.4 mM	.5 µM BFC, 72.5 mM sucrose, 45 mM, KPO_4, 1mM NADPH 0.384M APAP	.5 µM BFC, 72.5 mM sucrose, 45 mM, KPO_4, 1mM NADPH, 3.84mM APAP

Appendix D — SOP BFC Assay *A. annua* Tea IC_{50} Determination (rk)

BFC Assay

Reagents:

1. *Artemisia annua* tea Lot # containing 306 µM artemisinin.
2. 3.84 mM acetaminophen from Thermo Fisher Scientific #102330050
3. Ketoconazole from Cayman Chemical Company #51212
4. Methanol from Fisher Chemical Thermo Fisher Scientific #203403
5. 100 mM BFC solution: dissolved in DMSO Cayman Chemical Company #3572
6. 7.4 pH KPO_4 Buffer 0.9 M created with both potassium phosphate dibasic (BP363-500) and potassium phosphate monobasic anhydrous both sourced from Fisher Bioreagents.
7. Sucrose solution: 250 mM diluted in water and sourced from Sigma Aldrich
8. Distilled water
9. Human Liver Microsomes: sourced from Sekisui XenoTech #H2620 with a protein content of 20 mg/ml and a P450 content of 335 pmol/mg diluted with 250 mM sucrose #S-1888 to 0.2 µg/µL.
10. NADPH: 4 mM in NADPH in pH 8 10 mM Tris HCl
11. Tris buffer: 10 mM of Tris HCl #T-3253 from Sigma Aldrich diluted in water. The pH was adjusted to 8.0 with Trizma base #T1503-500G from Sigma Aldrich.

Tools:

6. 96-well white assay plate (flat bottom polystyrene) #33-754 from Genesee Scientific
7. Incubator set to 37°C
8. 1000, 200, 100, 20, and 2 µL micropipettes
9. Victor Nivo Plate Reader
10. Aquarium Air Pump

Procedure:

1. Removed KPO_4 from the 4°C refrigerator to warm to 25°C.
2. The *Artemisia annua* tea is serially diluted to a molarity of 1/8000 of the original
3. 40 µL of each tea dilution is pipetted into the wells
    a. Refer to the table below for amounts.
4. Human liver microsome (HLM) aliquots of 0.2 µg/µL are removed from the - 20 °C freezer.

5. Another analogous dilution series was created with each well containing 40 µL tea, 1 µL of BFC, 29 µL of sucrose, 5 µL of KPO_4 and 25 µL of NADPH. This will serve as the background control.
6. A master solution of 1 µL 100 mM BFC was diluted in 19 µL water for each well used. Then 5 µL of KPO_4 and 29 µL of HLM was added for each well used. The master solution was mixed by pipetting. 75 µL of mixture was pipetted into each well.
    g. There were typically 27 wells so a solution of 2.3 µL BFC was mixed with 43.9 µL of water
    h. One column received no inhibitor but had all of these reagents added via the master mixture.
7. The NMC was prepared separately with these three wells receiving 29 µL of sucrose, 45 µL of KPO_4 and 1 µL of the diluted BFC (and no ketoconazole) to create No Microsome Control (NMC).
8. The plate was then pre-incubated at 37°C for 5 minutes.
9. 25 µL of 4 mM NADPH (in 10 mM Tris buffer at pH 8) is added to each well by a multi-channel pipette to start the reaction.
10. Immediately after pipetting the NADPH into the wells the fluorescence was measured using the Victor NIVO.
11. The wells were then incubated at 37°C for 30 minutes.
12. The Fluorescence of the wells was then read via the Victor NIVO. At the start of the method development, the fluorescence of a well was compared to the fluorescence of a control well (Row D). For instance, fluorescence of A11 - D11 or Fluorescence of B9-D9. Later in the method development, the plate's fluorescence after the reaction and incubation was compared to the fluorescence right after the NADPH's addition (Fluorescence after incubation - Fluorescence immediately after the addition of NADPH).

Table 9: Table showing the contents of each well within a 96 well plate. Rows 4-11 are analytical wells. Columns 1 -3 contain NMC's and NIC's for further calculations and calibrations and a ketoconazole well for control.

Amount of Tea Artemisinin	Keto (0.5 µg per well)	NMC	NIC	0.000076 µM	0.00076 µM	0.0076 µM	0.0763 µM	0.763 µM	7.63 µM	15.3 µM	30.5 µM	61.1 µM	122 µM
	1	1	2	3	3	4	5	6	7	8	9	10	11
A	1 µL BFC, 29 µL HLM, 5 µL KPO_4, 25µL NADPH	1 µL BFC, 29 µL Sucrose, 5 µL KPO_4, 25µL NADPH	1 µL BFC, 29 µL HLM, 5 µL KPO_4, 25µL NADPH	1 µL BFC, 29 µL HLM, 5 µL KPO_4, 25µL NADPH	1 µL BFC, 29 µL HLM, 5 µL KPO_4, 25µL NADPH	1 µL BFC, 29 µL HLM, 5 µL KPO_4, 25µL NADPH	1 µL BFC, 29 µL HLM, 5 µL KPO_4, 25µL NADPH	1 µL BFC, 29 µL HLM, 5 µL KPO_4, 25µL NADPH	1 µL BFC, 29 µL HLM, 5 µL KPO_4, 25µL NADPH	1 µL BFC, 29 µL HLM, 5 µL KPO_4, 25µL NADPH	1 µL BFC, 29 µL HLM, 5 µL KPO_4, 25µL NADPH	1 µL BFC, 29 µL HLM, 5 µL KPO_4, 25µL NADPH	1 µL BFC, 29 µL HLM, 5 µL KPO_4, 25µL NADPH
B	1 µL BFC, 29 µL HLM, 5 µL KPO_4, 25µL NADPH	1 µL BFC, 29 µL Sucrose, 5 µL KPO_4, 25µL NADPH	1 µL BFC, 29 µL HLM, 5 µL KPO_4, 25µL NADPH	1 µL BFC, 29 µL HLM, 5 µL KPO_4, 25µL NADPH	1 µL BFC, 29 µL HLM, 5 µL KPO_4, 25µL NADPH	1 µL BFC, 29 µL HLM, 5 µL KPO_4, 25µL NADPH	1 µL BFC, 29 µL HLM, 5 µL KPO_4, 25µL NADPH	1 µL BFC, 29 µL HLM, 5 µL KPO_4, 25µL NADPH	1 µL BFC, 29 µL HLM, 5 µL KPO_4, 25µL NADPH	1 µL BFC, 29 µL HLM, 5 µL KPO_4, 25µL NADPH	1 µL BFC, 29 µL HLM, 5 µL KPO_4, 25µL NADPH	1 µL BFC, 29 µL HLM, 5 µL KPO_4, 25µL NADPH	1 µL BFC, 29 µL HLM, 5 µL KPO_4, 25µL NADPH
C	1 µL BFC, 29 µL HLM, 5 µL KPO_4, 25µL NADPH	1 µL BFC, 29 µL Sucrose, 5 µL KPO_4, 25µL NADPH	1 µL BFC, 29 µL HLM, 5 µL KPO_4, 25µL NADPH	1 µL BFC, 29 µL HLM, 5 µL KPO_4, 25µL NADPH	1 µL BFC, 29 µL HLM, 5 µL KPO_4, 25µL NADPH	1 µL BFC, 29 µL HLM, 5 µL KPO_4, 25µL NADPH	1 µL BFC, 29 µL HLM, 5 µL KPO_4, 25µL NADPH	1 µL BFC, 29 µL HLM, 5 µL KPO_4, 25µL NADPH	1 µL BFC, 29 µL HLM, 5 µL KPO_4, 25µL NADPH	1 µL BFC, 29 µL HLM, 5 µL KPO_4, 25µL NADPH	1 µL BFC, 29 µL HLM, 5 µL KPO_4, 25µL NADPH	1 µL BFC, 29 µL HLM, 5 µL KPO_4, 25µL NADPH	1 µL BFC, 29 µL HLM, 5 µL KPO_4, 25µL NADPH
D (Back-ground)				1 µL BFC, 29 µL Sucrose 5 µL KPO_4, 25µL NADPH	1 µL BFC, 29 µL Sucrose 5 µL KPO_4, 25µL NADPH	1 µL BFC, 29 µL Sucrose 5 µL KPO_4, 25µL NADPH	1 µL BFC, 29 µL Sucrose 5 µL KPO_4, 25µL NADPH	1 µL BFC, 29 µL Sucrose 5 µL KPO_4, 25µL NADPH	1 µL BFC, 29 µL Sucrose 5 µL KPO_4, 25µL NADPH	1 µL BFC, 29 µL Sucrose 5 µL KPO_4, 25µL NADPH	1 µL BFC, 29 µL Sucrose 5 µL KPO_4, 25µL NADPH	1 µL BFC, 29 µL Sucrose 5 µL KPO_4, 25µL NADPH	1 µL BFC, 29 µL Sucrose 5 µL KPO_4, 25µL NADPH
Final Concentrations	1 µL BFC, 29 µL HLM, 5 µL KPO_4, 25µL NADPH, 0.094 µM Keto	.5 µM BFC, 72.5 mM sucrose, 45 mM, KPO_4, 1mM NADPH	.5 µM BFC, 72.5 mM sucrose, 45 mM, KPO_4, 1mM NADPH	.5 µM BFC, 72.5 mM sucrose, 45 mM, KPO_4, 1mM NADPH 0.000076µM Tea Artemisinin	.5 µM BFC, 72.5 mM sucrose, 45 mM, KPO_4, 1mM NADPH 0.00076 µM Tea Artemisinin	.5 µM BFC, 72.5 mM sucrose, 45 mM, KPO_4, 1mM NADPH 0.00763 µM Tea Artemisinin	.5 µM BFC, 72.5 mM sucrose, 45 mM, KPO_4, 1mM NADPH 0.0763µM Tea Artemisinin	.5 µM BFC, 72.5 mM sucrose, 45 mM, KPO_4, 1mM NADPH 0.763µM Tea Artemisinin	.5 µM BFC, 72.5 mM sucrose, 45 mM, KPO_4, 1mM NADPH 7.63 µM Tea Artemisinin	.5 µM BFC, 72.5 mM sucrose, 45 mM, KPO_4, 1mM NADPH 15.3 µM Tea Artemisinin	.5 µM BFC, 72.5 mM sucrose, 45 mM, KPO_4, 30.5 µM Tea Artemisinin	.5 µM BFC, 72.5 mM sucrose, 45 mM, KPO_4, 61.1 µM Tea Artemisinin	.5 µM BFC, 72.5 mM sucrose, 45 mM, KPO_4, 1mM NADPH, 122 µM Tea Artemisinin